WEIDLINGER ASSOCIATES, CONSULTING ENGINEERS
110 EAST 59TH STREET
NEW YORK, NEW YORK 10022

and

SUITE 245, BUILDING 4
3000 SAND HILL ROAD
MENLO PARK, CALIFORNIA 94025

DEVELOPMENT OF INTERFERENCE RESPONSE SPECTRA FOR LIFELINES SEISMIC ANALYSIS

By

I. Nelson
P. Weidlinger

Interim Grant Report No. IR-2

Prepared for
National Science Foundation (RANN Branch)
1800 G Street
Washington, D.C. 20550

Grant No. ENV P76-9838

JULY 1, 1977

BIBLIOGRAPHIC DATA SHEET	1. Report No. NSF/RA-770313	2.	3. Recipient's Accession No. PB275215
4. Title and Subtitle Development of Interference Response Spectra for Lifelines Seismic Analysis (Interim Grant Report No. IR-2)			5. Report Date July 1, 1977 6.
7. Author(s) I. Nelson, P. Weidlinger			8. Performing Organization Rept. No. IR-2
9. Performing Organization Name and Address Weidlinger Associates, Consulting Engineers 110 East 59th Street New York, NY 10022			10. Project/Task/Work Unit No. 11. Contract/Grant No. ENVP769838
12. Sponsoring Organization Name and Address Research Applied to National Needs (RANN) National Science Foundation Washington, D.C. 20550			13. Type of Report & Period Covered Interim 14.

15. Supplementary Notes

16. Abstracts The authors contend that the dynamic response of a pipe network system may be determined by numerical integration of the appropriate equations of motion. An important criterion for failure of underground pipes subjected to seismic loading is the strain, or difference in displacement, between two points along the pipe. The concept of interference spectrum has been introduced to deal with this problem when dynamic effects are significant. The approach required to analyze a multi-degree of freedom pipe network is outlined. The case of only two connected pipes segments is treated in detail, and shown to be equivalent to a single degree of freedom system. The mathematical treatment is described in detail and the computer code developed is described. Numerical results are presented for both the El Centro 1940 and 15250 Ventura Boulevard 1971 input records. Results demonstrate that it may be possible to estimate, or at least bound, interference spectrum without actually computing it. Finally, it is noted that, for long periods, the absolute velocity spectrum is approximately the same as the pseudo-velocity spectrum, which in turn is readily available for most earthquakes.

17. Key Words and Document Analysis. 17a. Descriptors

Earthquakes
Pipes (tubes)
Line pipes
Pipelines
Piping systems
Seismology
Earthquake resistant structures

17b. Identifiers/Open-Ended Terms

Lifelines
Seismic analysis
Interference Response Spectra

17c. COSATI Field/Group

18. Availability Statement NTIS	19. Security Class (This Report) UNCLASSIFIED	21. No. of Pages 47
	20. Security Class (This Page) UNCLASSIFIED	22. Price PC03/MF01

CAPITAL SYSTEMS GROUP, INC.
6110 EXECUTIVE BOULEVARD
SUITE 250
ROCKVILLE, MARYLAND 20852

INTERFERENCE RESPONSE SPECTRA

I INTRODUCTION

Pipelines subjected to an earthquake are affected by the ground shaking. The motion may be described as a function of time (t) and a space coordinate (x) measured along the axis of the pipe. The resulting displacement field

$$x_G = x_G\,(x,t) \tag{1}$$

is given at a point, chosen as the origin,and its temporal and spatial variation along the x coordinate may be considered as the sum of the following effects:

a) phase angle shift due to wave propagation delay,

b) variation of wave form due to gross change in base rock formation (slope, elevation, etc.),

c) variation casued by gross change in overburden soil properties and layering,

d) purely random local variation definable only by statistical parameters (mean value, variance, correlation distance).

The ground displacement field is a subject of current investigation, but if for the purposes of this paper we assume it to be known, the dynamic response of a pipe network system may be determined by numerical integration of the appropriate equations of motion. Such calculations (by means of a finite element model) are currently in progress, but because of their expensive and time-consuming nature, they are not appropriate for the routine analysis of pipe network components. The results of these structure-medium interaction studies, however, are useful in the construction of simpler, discrete models. In these, the network is represented

by rigid (or elastic) links interconnected by (elastic or inelastic) springs and dashpots. The system is reacted by a Winkler foundation consisting of discrete springs and dashpots, capable of transmitting axial (or transverse) displacements (Fig. 1). In this discrete model, the soil-structure interaction behavior is incorporated in terms of virtual mass, effective stiffness and radiation and material damping. It may also include elements representing friction and slippage. In the cases when such a model exhibits real frequencies and mode shapes, its dynamic response to ground excitation may be adequately treated by familiar response spectrum techniques. The purpose of this paper is to outline such methods.

II SINGLE DEGREE OF FREEDOM MODEL

The pipe network system of Fig. 1 may be represented to any degree of accuracy desired by an equivalent lumped mass system. For example, if only axial motion were of interest, the mass center of each link could be used to define the displacement field. The natural frequencies and associated mode shapes could then be found by standard techniques. The input for each mode would consist of a linear combination of the ground motion at the various node points.

Consider, for the moment, the simpler problem of only two pipe sections connected by a joint, represented by the previously described discrete model, and subjected to ground excitation x_{G1} and x_{G2} at two points separated by a distance L (Fig. 2). This model is equivalent to a damped linear oscillator of two degrees of freedom, as shown in Fig. 3. The constants k_p, c_p and m represent the stiffness, damping and mass (including virtual effects) of the pipes and joints, while k_g and c_g are the stiffness and damping quantities associated with soil-structure interaction.

The equations of motion of the system are

$$m\ddot{x}_1 = k_p\,(x_2-x_1) - k_g\,(x_1-x_{G1}) + c_p\,(\dot{x}_2-\dot{x}_1) - c_g\,(\dot{x}_1-\dot{x}_{G1}) \tag{2}$$

$$m\ddot{x}_2 = -k_g\,(x_2-x_{G2}) - k_p\,(x_2-x_1) - c_g\,(\dot{x}_2-\dot{x}_{G2}) - c_p\,(\dot{x}_2-\dot{x}_{G2}) \tag{3}$$

The system exhibits two modes of free vibration. By adding Eqs (2) and (3) (and rearranging terms), one obtains

$$m(\ddot{x}_1+\ddot{x}_2) + c_g(\dot{x}_1+\dot{x}_2) + k_g(x_1+x_2) = k_g(x_{G1}+x_{G2}) + c_g(\dot{x}_{G1}+\dot{x}_{G2}) \tag{4}$$

which is the equation of motion of the rigid body mode where the distance L between the two mass points remains constant. This mode is of no interest because it causes no strain in k_p representing the stiffness of the pipe-joint system. The second mode, which produces strain in both k_p and k_g may be found by subtracting Eqs (2) and (3), i.e.

$$m(\ddot{x}_1-\ddot{x}_2) + (c_g+2c_p)\,(\dot{x}_1-\dot{x}_2) + (k_g+2k_p)\,(x_1-x_2) = k_g\,(x_{G1}-x_{G2}) + c_g\,(\dot{x}_{G1}-\dot{x}_{G2}) \tag{5}$$

or

$$\Delta\ddot{x} + 2\beta\bar{\omega}\Delta\dot{x} + \bar{\omega}^2\Delta x = \frac{k_g}{m}\,(x_{G1}-x_{G2}) + \frac{c_g}{m}\,(\dot{x}_{G1}-\dot{x}_{G2}) \tag{6}$$

where

$$\Delta x = x_1 - x_2 \tag{7}$$

$$\bar{\omega} = \sqrt{\frac{k_g + 2k_p}{m}} \tag{8}$$

and

$$\beta = \frac{(c_g + 2c_p)}{2m\bar{\omega}} \tag{9}$$

Equation (6) represents the equation of motion of a single degree of freedom system with undamped circular frequency $\bar{\omega}$ and damping ratio β.

If the input motion is specified in terms of ground acceleration, it is convenient to rewrite Eq (6) as

$$\ddot{y} + 2\beta\bar{\omega}\dot{y} + \bar{\omega}^2 y = -\alpha(\ddot{x}_{G1} - \ddot{x}_{G2}) - \frac{1}{m}\left[\alpha\,(c_g + 2c_p) - c_g\right](\dot{x}_{G1} - \dot{x}_{G2}) \tag{10}$$

where y is the "relative" displacement

$$y = \Delta x - \alpha(x_{G1} - x_{G2}) \tag{11}$$

and

$$\alpha = (1 + 2k_p/k_g)^{-1} \tag{12}$$

In the case when $c_p/c_g = k_p/k_g$, the second term on the right hand side of Eq. (10) drops out. Alternately, if α is close to unity, and $c_p/c_g \ll 1$ (pipe and joint damping is much less than that of the soil), the second term will be extremely small. Without any great loss of generality, the second term will be neglected, yielding

$$\ddot{y} + 2\beta\bar{\omega}\dot{y} + \bar{\omega}^2 y = -\ddot{\bar{x}}_G \tag{13}$$

where

$$\bar{x}_G = \alpha(x_{G1} - x_{G2}) \tag{14}$$

Equation (13) is the standard differential equation for the relative motion of a single degree of freedom oscillator with damping, except the input here represents the difference in ground acceleration at two points, reduced by the factor α.

In the subsequent treatment we will illustrate the case of interference due to a phase angle shift across the separation distance L, caused by a time delay Δt, defined by

$$L = C_s \Delta t \tag{15}$$

where C_s is the local velocity of wave propagation in the soil. The forcing function, therefore, becomes

$$\bar{x}_G = \alpha\left[x_G(x,t) - x_G(x+L,t)\right] \tag{16}$$

Since the displacements may be assumed to propagate in an elastic medium, they satisfy an equation of the form

$$x_G(x,t) = f(x-C_s t) \tag{17}$$

so that the equivalent forcing function $\bar{x}_G$ can be given as

$$\bar{x}_G = \alpha\left[x_{G1}(t) - x_{G1}(t+\Delta t)\right] \tag{18}$$

Neglecting α for the moment, Eq. (13) may be used to construct a frequency response spectrum of the second mode motion of the system shown in Fig. 3 and given by Eqs (2) and (3). This spectrum (to distinguish it from its standard form) is referred to as an Interference Response Spectrum, and it is given in terms of the frequency $\bar{\omega}$ and a spectral amplitude $\bar{S}$ defined so that

$$S = \alpha\bar{S} \tag{19}$$

where S is the amplitude corresponding to the response of the original system.

To obtain the actual amplitude the value of the spectral amplitude is multiplied by the constant

$$\alpha = (1+2k_p/k_g)^{-1} \leq 1 \qquad \text{(see Eq. 12)}$$

An upper bound to S occurs when the stiffness of the pipe system is negligible compared to that of the equivalent soil spring constant, i.e. $\alpha = 1$.
The amplitude response is also dependent on the delay time Δt. The spectrum $\bar{S}(\bar{\omega},\Delta t)$ thus is given as a family of curves with the parameters Δt, which in turn define the distances L as given by Eq. 15.

III MULTIPLE DEGREE OF FREEDOM SYSTEMS

The real problem of interest is that represented by Fig. 1, which may exhibit many independent mode shapes and frequencies. A system of equations, which in matrix form appear similar to Eq (13), may be set up to represent the physical system. If we assume modal damping, then an equation for a single degree of freedom system may be written for each mode. It would appear that with $\bar{\omega} \rightarrow \omega_n$, the frequency of the nth mode, the interference spectrum could be used directly to predict the response of that mode. However, it should be noted that, in general, the forcing function for the nth mode would contain the ground motion of every segment along the structure. Thus, there would not be a unique length L, or delay time Δt, required to define the interference spectrum. Nevertheless, it may be possible to represent an equivalent length (or Δt) in terms of the dominant wavelength of the particular mode.

The development of the spectrum for actual ground motion records is given in the subsequent sections. The application and some of its consequences will be reported in a subsequent paper.

IV. INPUT GROUND MOTION

Approximately 300 earthquake ground motion records are available from the Earthquake Engineering Research Laboratory. Copies of Vol. II, which contain the processed acceleration records, as well as integrated velocity and displacement records, were obtained on magnetic tape so that various hypotheses could be checked by computational experiments. The records are in a standard format in which the acceleration values are given every 0.02 sec, the velocity every 0.04 sec, and the displacement every 0.10 sec.

To gain experience in reading the tapes and processing the data, a simple program was developed which read the digitized acceleration record, and then computed velocity and displacement records by numerical integration using the trapezoidal rule. Both the initial velocity and displacement were assumed to be zero. The computed velocity and displacement records, were then compared with those given on the tape. Figure 4 shows the displacement time histories of the May 18, 1940 El Centro record, S00E component, obtained by integration and directly from the tape. Clearly, there is a problem of a baseline adjustment. It was noted that the first values of both the velocity and displacement on the tape record were non-zero.

This problem was discussed with Prof. M.D. Trifunac, currently at the University of Southern California, who was responsible for processing and adjusting the raw accelerogram records. Prof. Trifunac explained that $t = 0$ is not the beginning of the motion; rather, it is the time at which the acceleration reaches a sufficient magnitude to trigger the recording mechanism. Therefore, a non-zero "initial" velocity (or displacement) results from baseline adjusting the entire record; i.e., the initial velocity is the velocity at $t = 0$ required such that the velocity at the end

of the record oscillates about zero. In addition, Prof. Trifunac pointed out that the velocity record (on tape) is not strictly the integral of the acceleration, and the displacement is not strictly the integral of the velocity. This is true because each of the three records is filtered independently in the frequency domain.

To develop interference spectra, consistent finely spaced acceleration, velocity and displacement records are needed, i.e., records in which $dx/dt = v$ and $dv/dt = a$. Following Prof. Trifunac's suggestion, the adjusted acceleration is viewed as the basic record. The trapezoidal integration scheme with $\delta t = 0.02$ sec is sufficiently accurate. However, the initial velocity and displacement are those given on the tape. The velocity and displacement waveforms of the 1940 El Centro S00E record obtained in this manner are compared with those directly from the tape in Figs. 5 and 6, respectively. While the curves, especially the displacements, do not correspond exactly, they are sufficiently close to use.

V. COMPUTER PROGRAM

Initially, the physical model may be viewed as that shown in Fig. 3, with k_p and c_p both going to zero. The inputs x_{G1} and x_{G2} are the ground motion at two points along the pipe. The parameters k, c and m (assumed identical at both points) could represent the interaction of say a junction box along the pipe with the ground, while k_p and c_p are assumed to be the vanishingly small axial stiffness and damping of the jointed pipe. The quantity $x_1 - x_2$ represents the stretching of the pipe. When the maximum value of $|x_1 - x_2|/L$, where L is the length of pipe between points 1 and 2, reaches a critical strain, failure is likely to occur. While only the case of $\alpha = 1$ will be considered here, the extension to $\alpha < 1$ would follow easily as discussed previously.

A computer program DFSPECT was written to compute interference spectra, i.e., $\max|x_1(t) - x_2(t)|$ as a function of $\omega = \sqrt{k/m}$. The basic subroutine SPECTD was a modification of a spectra subroutine developed for our explosion induced ground shock work. The routine solves the differential equation for a single degree of freedom system (with damping)

$$\ddot{y} + \frac{c}{m}\dot{y} + \frac{k}{m}y = -\ddot{x}_G \tag{20}$$

where $y = x - x_G$ is the relative displacement, and where $\ddot{x}_G$ is the input ground acceleration record. The input acceleration is assumed to vary linearly within a time step δt, i.e.,

$$\ddot{x}_G(t) = a_0 + (a_1 - a_0)\frac{t}{\delta t} \quad , \quad t_0 \leq t \leq t_0 + \delta t \tag{21}$$

The relative displacement and velocity at the beginning of the time step, $t = t_0$, are Y_{OLD} and V_{OLD}, respectively. Equation (20) is solved exactly for each time step, i.e.,

$$y(t_0 + \delta t) = e^{-\beta\omega\delta t}\left[C_{coef}\cos\omega_c\delta t + S_{coef}\sin\omega_c\delta t\right] - \frac{a_1}{\omega^2} + \frac{2\beta}{\omega^3}\frac{(a_1 - a_0)}{\delta t} \tag{22}$$

where β = fraction of critical damping $= \frac{c}{2m\omega}$

$\omega = \frac{2\pi}{f} = \sqrt{\frac{k}{m}} =$ circular frequency of the system without damping

$\omega_c = \omega\sqrt{1 - \beta^2} =$ circular frequency of the damped system (23)

C_{coef} and S_{coef} are the coefficients of the Cosine and Sine terms in Eq. 22, i.e.,

$$C_{coef} = Y_{OLD} + \frac{a_0}{\omega^2} - \frac{2\beta}{\omega^3}\frac{(a_1 - a_0)}{\delta t}$$

$$S_{coef} = \frac{\beta\omega\, C_{coef} + V_{OLD} + \dfrac{(a_1 - a_0)}{\omega^2\delta t}}{\omega_c} \tag{24}$$

The corresponding relative velocity is

$$\dot{y}(t_0 + \delta t) = e^{-\beta\omega\delta t} \left\{ \begin{array}{l} C_{coef} \left[-\beta\omega \cos \omega_c \delta t - \omega_c \sin \omega_c \delta t \right] \\ \\ + S_{coef} \left[\omega_c \cos \omega_c \delta t - \beta\omega \sin \omega_c \delta t \right] \end{array} \right\} - \frac{(a_1 - a_0)}{\omega^2 \delta t} \quad (25)$$

The results of Eqs. (22) and (25) are then used as new initial conditions, Y_{OLD} and V_{OLD}, and the Eqs. (22) and (25) are then solved for the next time step.

The maximum value of $|y(t)|$ is the standard or relative spectral displacement at frequency $\omega/2\pi$. When the period

$$T = \frac{1}{f} = \frac{2\pi}{\omega} >> \delta t \quad (26)$$

the maximum value $|Y_{OLD}|$ is sufficiently close to the maximum of $|y(t)|$ to be used as the spectral value. A factor of four for $T/\delta t$ is used for Eq. (26) in the program. If $T/\delta t < 4$, no spectral calculations are made. With the earthquake acceleration records, the time interval of the data, $\delta t = 0.020$ sec, results in a minimum period T of 0.080 sec, or a maximum credible frequency of 12.5 Hz.

It is possible that the peak value of $|y|$, for a certain ω occurs after the final time of the input base motion. The acceleration time history is postulated to be zero for $t > t_f$, and the free vibration problem is then solved with the maximum value of $|y|$ found analytically. This value is compared with the value found for $t \leq t_f$. For the rather long earthquake records, $t_f > 30$ sec, and with almost any damping, the value computed during free vibration seldom governs.

While the program searches for the maximum relative displacement, it also finds the time at which it occurs (either during the record or during free vibration). Similarly, the maximum relative velocity $|\dot{y}|_{max}$ and the

time at which it occurs are recorded. In general, this relative velocity spectra is not equal to the so-called pseudo-velocity, $\omega\left|y\right|_{max}$. Rather than compute the peak relative acceleration, at this point in the program the psuedo-acceleration, the value of $\omega^2\left|y\right|_{max}$ is recorded. Values of $\left|y\right|_{max}$, $\left|\dot{y}\right|_{max}$, $\omega^2\left|y\right|_{max}$ and their times of occurrences (as functions of frequency), as well as th pseudo-velocity are printed out and stored on magnetic tape for later processing.

The input ground motion consists of the digitized acceleration record as well as its first and second integrals obtained previously using the trapezoidal rule. The initial velocity and displacement were those on the tape, as discussed previously.

For each frequency and during each time step in the calculation, the value of the ground displacement and velocity are added to Y_{OLD} and V_{OLD}, respectively, to obtain the time history of the absolute motion of the mass. The absolute acceleration of the mass is evaluated from the equation of motion, Eq. (20), i.e.,

$$a_n = \ddot{y} + \ddot{x}_G = - \omega^2 y_n - 2\beta\, \omega \dot{y}_n \tag{27}$$

The complete time histories of the absolute motion of the mass are thus available for each frequency. The maximum values (without regard to sign) are defined as the absolute displacement, velocity and acceleration spectra. Their values and times of occurrence are printed out and recorded on magnetic tape for later processing.

The object of this phase of the study is to develop and analyze interference spectra. In general, ground motions are available at isolated sites. Our interest is in differences in motion at adjacent sites. As a first approximation, one can assume that the same ground motion occurs at two adjacent points a distance L apart, but shifted in time an amount

$\Delta t = L/C$, where C is an "appropriate" wave velocity*). Values of Δt are read in and interference spectra are computed for each.

Once the time history of the absolute motion of a single mass on a spring-dashpot is available (i.e., $x(t_n)$, $v(t_n)$, $a(t_n)$, n = 1, N), interference spectra are easily computed. This is done in subroutine DSPEC. The interference displacement, velocity and acceleration spectra for each frequency are defined respectively as

$$\begin{aligned} &\max\left|x(t_n) - x(t_n - \Delta t)\right| \\ &\max\left|v(t_n) - v(t_n - \Delta t)\right| \\ &\max\left|a(t_n) - a(t_n - \Delta t)\right| \end{aligned} \tag{28}$$

To compute $v(t_n - \Delta t)$ and $a(t_n - \Delta t)$ when Δt is not an exact multiple of the 0.020 sec time spacing, linear interpolation is used. However, since the prime interest is in differential displacements, and since values of Δt on the order of the 0.02 sec spacing were anticipated, a higher order interpolation scheme was used for computing the displacement $x(t_n - \Delta t)$, i.e.,

$$\begin{aligned} x(t_n - \Delta t) = {} & \Delta\tau_2\, x_{j-1} + \Delta\tau_1\, x_j + \Delta\tau_1\, \Delta\tau_2\, (v_{j-1} - v_j)\, (t_j - t_{j-1}) \\ & + \frac{1}{2}\, \Delta\tau_1\, \Delta\tau_2\, (a_{j-1}\, \Delta\tau_1 + a_j\, \Delta\tau_2)\, (t_j - t_{j-1})^2 \end{aligned} \tag{29}$$

where $$t_{j-1} < t_n - \Delta t < t_j \tag{30}$$

$$\Delta\tau_1 = \frac{t_n - \Delta t - t_{j-1}}{t_j - t_{j-1}} \tag{31}$$

*) If a phase velocity-frequency diagram were available, the appropriate C would be $C(\omega)$. Incorporating this modification would not be difficult.

and $$\Delta\tau_2 = \frac{t_j - t_n + \Delta t}{t_j - t_{j-1}} \tag{32}$$

The error in Eq. (29) is bounded

$$\text{Error} \leq \frac{1}{96} \ddot{a}_{j-\frac{1}{2}} (t_j - t_{j-1})^4 \tag{33}$$

Mention should be made of the special treatment given late and early times, i.e., $t > t_f$ and $t < \Delta t$. The original ground motion data is extended somewhat before computing the spectra. In general, the last velocity (integrated acceleration) value will not be zero. The ground velocity is assumed to go to zero with a constant acceleration of approximately 0.01 g, and within ten additional time steps. Moreover, for an additional number of time steps corresponding to the maximum Δt, the ground velocity and acceleration are both set equal to zero, while the ground displacement is held constant. In this fashion, the interference spectrum may be computed with the standard algorithm described above, and with no special coding for late times, except checking the case when both oscillators are vibrating freely (a call to subroutine FREVIB with appropriate initial conditions).

The situation at early times is somewhat less satisfactory. The initial velocity and displacement of the ground motion are non-zero, while the initial conditions of the oscillator are unknown. If one assumes them to be zero, then the initial conditions Y_{OLD} and V_{OLD} at the first time step used to compute the relative motion, Eqs. (22) and (25), are non-zero. For high frequencies, these arbitrary initial discontinuities govern the spectra, and the results are seriously in error. Assuming the initial conditions of the oscillator and the ground to be identical, i.e., homogeneous conditions for the relative motion, is somewhat more satisfactory. The resulting (standard) relative spectra agrees with published results. However, a problem still exists in computing

interference spectra when Δt is on the order of the time step δt. The motion of the second oscillator must be defined for $t < \Delta t$. Recalling, $x_2(t) = x_1(t - \Delta t)$, the motion of x_1 must be given for $-\Delta t \leq t \leq 0$.

At first, thought was given to trying to extrapolate backwards in time using, say, a linearly varying acceleration. However, for that to work, the first value of ground acceleration, velocity and displacement must all have the same sign. A glance at only a few records shows this to be the exception rather than the rule.

The final solution was to alter the usual spring-dashpot model to a spring-dashpot-stick model. The model is rigid for $t \leq 0$ (i.e., ground motion and oscillator motion are identical for $t \leq 0$). At $t = 0$ the stick is removed so that the model is the usual one for $t > 0$. In the interference spectra calculation the motion of mass two for $t < \Delta t$ is assumed to be constant and given by the initial values of the ground motion (never mind the inconsistency!) In this manner the artificial initial conditions do not affect the results.

VI. DISCUSSION OF RESULTS

Relative, absolute and interference spectra were computed for the El Centro May 1940 S00E record. Initially, the values of Δt used for the interference spectra were 0.020, 0.100 and 0.50 sec. Computations were made for zero, 5 and 10% of critical damping. The spectra were printed and also stored for later plotting. Selected results are given below.

The standard tripartite plot of the relative spectra is shown in Fig. 7 for all three damping ratios. The envelope drawn on the figure corresponds to the undamped case. The unconnected circle at f = 0.158 Hz is not a plotting error; the peak undamped relative displacement at this frequency (and the peak for all frequencies) occurred at t = 55.449 sec, beyond the 53.74 sec duration of the record. This was one of the few places where the peak occurred during free vibrations. The plot tells us this by not connecting the point with the adjacent ones. There are 60 evenly spaced frequencies on the figure, from 0.052 to 12.02 Hz. While the undamped spectra are somewhat erratic, the damped cases are fairly smooth and taking more (or fewer) frequencies in the interval would most likely make little difference in the curves. Likewise, only a moderate change in the spectra occur when the damping ratio is increased from 5 to 10%. The envelope values for all three cases are given below:

Variation of Bounding Values with Damping

Damping Ratio %	Relative Displacement (cm)	Relative Velocity (cm/sec)	Pseudo-Velocity (ωD) (cm/sec)	Absolute Acceleration (g's)	Pseudo-Acceleration ($\omega^2 D$) (g's)
0	64.79	248.27	243.63	3.174	3.174
5	40.93	90.59	80.43	0.919	0.922
10	32.17	67.96	65.99	0.753	0.735

The relative displacement spectra is plotted directly against the period in Fig. 8, again for all three damping ratios. The relative displacement becomes very small for very stiff systems, i.e., for short periods. The absolute displacement spectra are plotted in Fig. 9. Here, for all damping ratios, the spectra at short periods reduce to the maximum ground displacement of 12.6 cm occurring at t ≃ 8.6 sec, see Fig. 6. The absolute and relative displacement spectra, for the 5% damping ratio, are compared in Fig. 10, this time plotted to a linear scale. Other than the fact that the curves cross, there does not appear to be much one can say about them.

The relative velocity spectra, for all three damping ratios, are shown in Fig. 11, while the absolute velocity spectra are given in Fig. 12. For short periods, the absolute velocity speetra is ≃ 36 cm/sec and occurs at t = 2.18 sec, the time of the peak velocity in the ground motion, see Fig. 5. The relative spectra at long periods reaches a somewhat greater value ≃ 38 cm/sec at the same time. The relative, absolute and pseudo-velocity spectra, for 5% of critical damping, are plotted against each other in Fig. 13. For short periods, the pseudo-velocity and relative velocity spectra are very similar. At mid-frequencies, near where maximum velocity enhancement occurs, all three curves are similar. For long periods (or low frequencies) the pseudo-velocity and absolute velocity are very similar, and substantially below the relative velocity spectra. The same three curves are plotted to a linear scale in Fig. 14.

The interference displacement spectra, for all three damping ratios, and for Δt = 0.020, 0.100 and 0.500 sec, are shown in Figs. 15, 16 and 17, respectively. They are compared with 5% of critical damping, on a linear scale in Fig. 18, and on a log scale in Fig. 19. Also shown as dashed lines on Fig. 19 are the absolute velocity spectra multiplied by the respective values of Δt. The limit, as $\Delta t \to 0$, of the interference displacement spectra

should approach the absolute velocity spectra (V_s) times Δt. This, in fact, occurs in Fig. 19 for $\Delta t = 0.020$ sec. For $\Delta t = 0.100$ sec, the two curves differ slightly only for short periods, on the order of Δt. For the highest value of Δt, the interference displacement spectra is substantially below $V_s \Delta t$, except for long periods.

Interference spectra were computed for three additional delay times to ascertain the trend for long Δt. The results for $\Delta t = 1.0$, 2.0, and 2.5 sec, together with the previous largest value, 0.5 sec, are shown in Fig. 20 (for 5% damping). While the interference displacement spectra are roughly proportional to Δt for long periods, $T > 5$ sec, the pattern no longer holds for short periods, $T < 5$ sec. In fact, for periods of approximately 2.5 sec, on the order of the largest delay time, the spectra for $\Delta t = 2.5$ sec is less than the other three curves. Clearly, the auto correlation function of the original ground motion forcing function must be related to this behavior.

It is also interesting to note that the interference displacement spectra for very high frequencies (at essentially zero period) are bounded by slightly more than 1 1/2 times the maximum free-field displacement of 12.5 cm. Moreover, 1 1/2 times the absolute displacement spectra appears to be a reasonable estimate of the interference displacement spectra for large Δt, while twice the absolute spectral value appears to be a reasonable upper bound. The interference spectra shown in Fig. 20 are replotted to a log scale in Fig. 21 with a band representing 1 1/2 to 2 times the absolute displacement spectra superimposed. The peaks of the interference spectra fall within the band.

This result is not too surprising. If the input ground motion were a pure sinusoid (which it is not), a time shift of a half period would double the response due to ΔX_G relative to that due to X_G itself. Any other time

shift would result in a smaller amplification.

Finally, some of the tentative conclusions were checked by performing the calculations with a different input earthquake record. The record chosen was the N79W component of the accelerogram recorded in the basement of 15250 Ventura Boulevard, Los Angeles, during the San Fernando earthquake of February 9, 1971. In passing, it should be mentioned that some waterpipe failures occurred along Ventura Boulevard during this earthquake. The N79W component is the component (essentially) parallel to the pipes that failed.

The relative, absolute and pseudo-velocity spectra, for 5% of critical damping are plotted (to a log scale) versus period in Fig. 22. While the comparable plot with the El Centro record (Fig. 13) exhibited a triple peak, a single peak at $T \simeq 2.5$ sec appears in Fig. 22. Nevertheless, the trends mentioned earlier apply here as well. The relative, absolute and pseudo-velocity, for 10% damping, are plotted to a linear scale against period in Fig. 23.

The interference spectra for this record were computed for $\Delta t = 0.02$, 0.10, 0.5 and 2.5 sec. The results (for 5% damping) are plotted to a linear scale against period in Fig. 24. As was the case in Fig. 20, the spectra are roughly proportional to Δt for long periods, but substantially reduced for periods on the order of Δt, or less. This is evident in Fig. 24 at $T \simeq 2.5$ sec, where the $\Delta t = 2.5$ sec curve drops below that for $\Delta t = 0.5$ sec.

The same spectra are plotted to a log scale in Fig. 25. Also shown as dashed lines in Fig. 25 for the three smallest values of Δt, and for $T > 4$ sec for $\Delta t = 2.5$ sec, are the values of the absolute velocity spectra time Δt. As was true in Fig. 19 for the El Centro record, for $\Delta t = 0.02$ sec, the curve $V_s \Delta t$ is indistinguishable from the corresponding interference displacement spectra. For $\Delta t = 0.10$ sec, while one can observe two distinct curves, at

least for short periods, the curves are even closer than the corresponding pair in Fig. 19. The two curves deviate for $\Delta t = 0.5$ sec, especially for periods $T \simeq \Delta t$. Finally, for the largest value of Δt, 2.5 sec, the interference spectra is substantially below $V_s \Delta t$ for most of the frequency range of interest. On the other hand, the shaded band, spanning the range from 1 1/2 to 2 times the absolute displacement spectra, includes (or bounds) the interference spectra for the largest value of Δt.

VII. SUMMARY AND CONCLUDING REMARKS

An important criterion for failure of underground pipes subjected to seismic loading is the strain or difference in displacement, between two points along the pipe. The concept of interference spectrum has been introduced to deal with this problem when dynamic effects are significant. The interference spectrum is the response S (the maximum difference in displacement) as a function of frequency $\bar{\omega}$ and delay time Δt. The present approach is limited to problems which may be treated as linear. The concept is applicable wherever the spatial variation of ground motion input is known. In this paper, the numerical examples are restricted to deal with only a shift of phase angle between adjacent points. Variation in ground motion due to changes in local geology are not included.

The approach required to analyse a multi-degree of freedom pipe network is outlined, although some uncertainty exists in the appropriate choice of delay time Δt. The case of only two connected pipes segments is treated in detail, and shown to be equivalent to a single degree of freedom system. While actual calculations have been limited to the case when the pipe/joint stiffness is much smaller than the ground stiffness, i.e., $\alpha = 1$, extension to the more general case $\alpha < 1$ is trivial. The mathematical treatment is described in detail and the computer code developed to solve them is

described. Numerical results are presented for both the El Centro 1940 and 15250 Ventura Boulevard 1971 input records.

The absolute velocity spectra, times the delay time Δt, is an excellent estimate of the interference spectra for small values of the delay time. For the limiting case of $\Delta t \to 0$, the relation is an exact one. For large values of Δt, those on the order of the predominant periods of the input record, twice the absolute displacement spectrum is a reasonable upper bound to the interference spectra,while 1 1/2 times the absolute spectrum appears to be a reasonable estimate. Thus, it may be possible to estimate, or at least bound, interference spectrum without actually computing it. Finally, it should be noted that for long periods the absolute velocity spectrum is approximately the same as the pseudo-velocity spectrum, which in turn is readily available for most earthquakes.

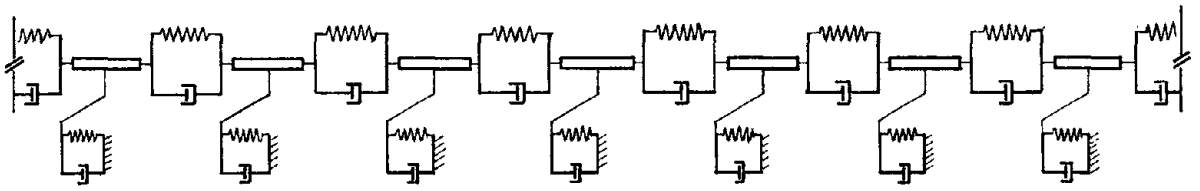

FIG. 1 LONG JOINTED PIPE SUPPORTED BY SPRINGS AND DASHPOTS

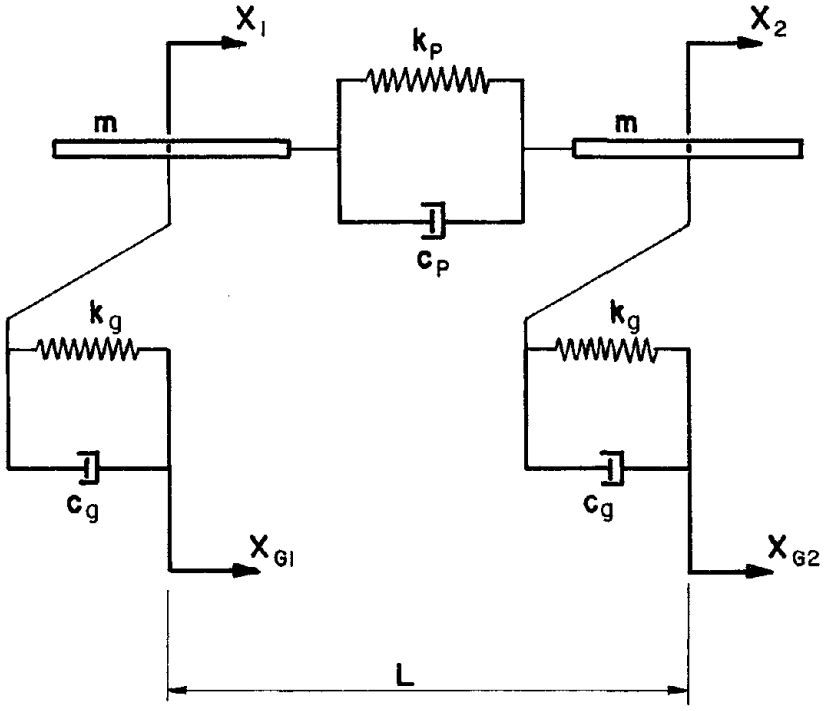

FIG. 2 TWO UNDERGROUND PIPE SEGMENTS CONNECTED BY JOINT

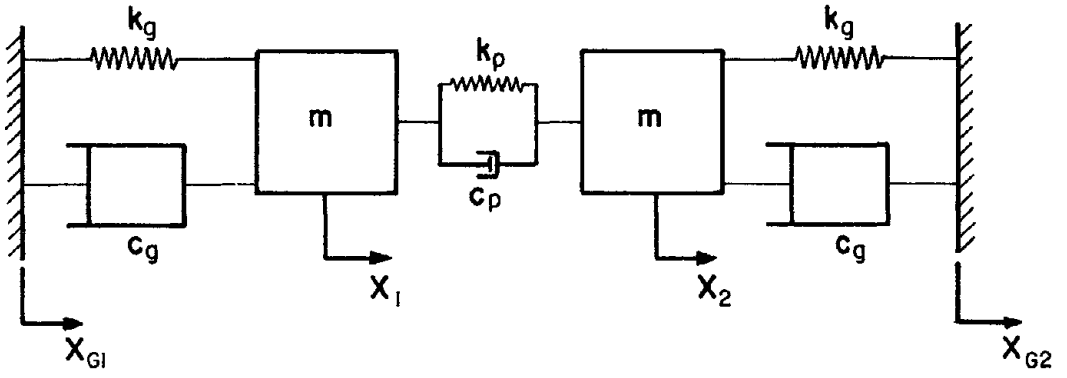

FIG. 3 LINEAR OSCILLATOR WITH TWO DEGREES OF FREEDOM

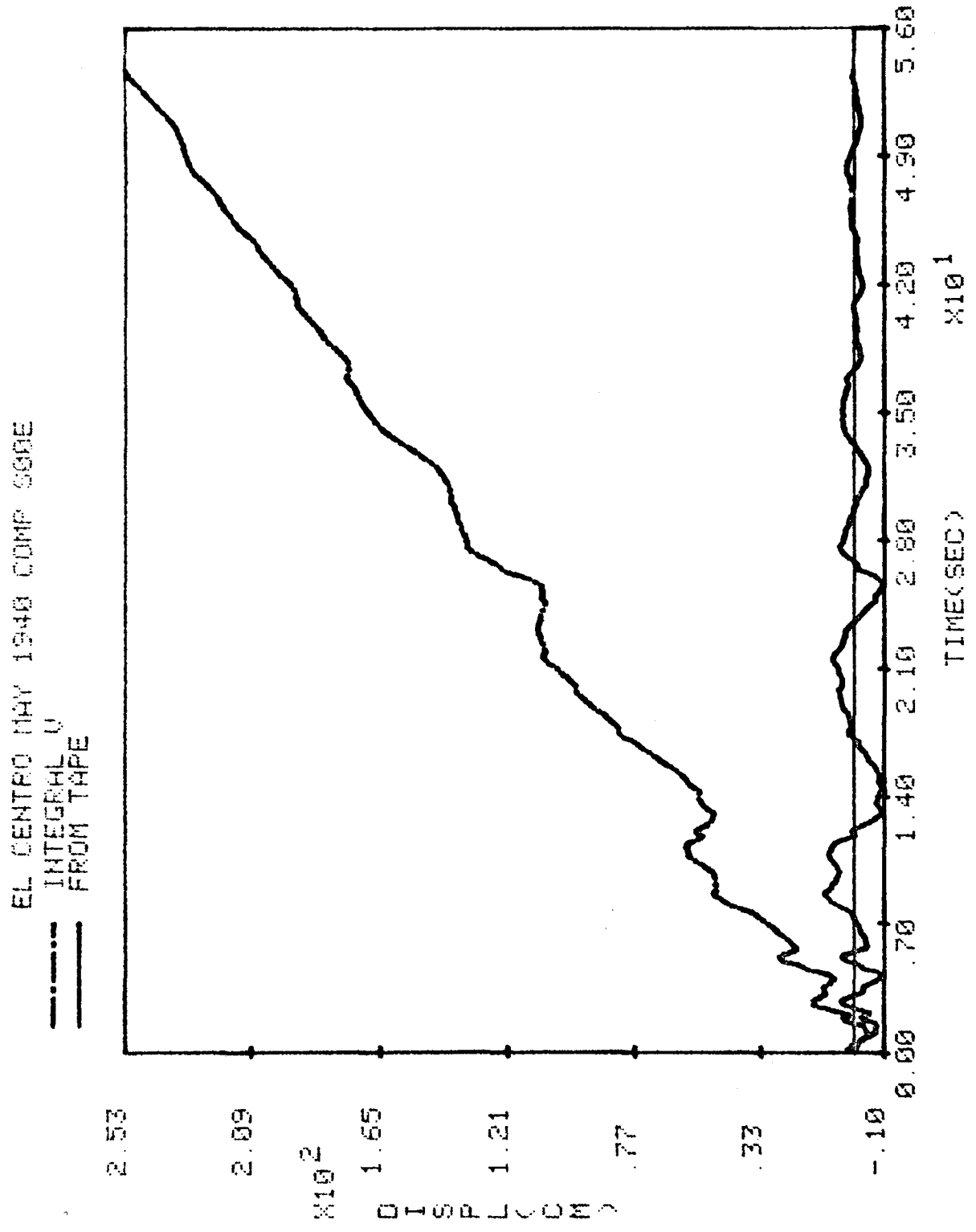
EL CENTRO NAY 1940 COMP S00E
INTEGRAL V
FROM TAPE
X10 2
DISPL(CM)
2.53
2.09
1.65
1.21
.77
.33
-.10
0.00
.70
1.40
2.10
2.80
3.50
4.20
4.90
5.60
TIME(SEC)
X10 1

FIG. 4

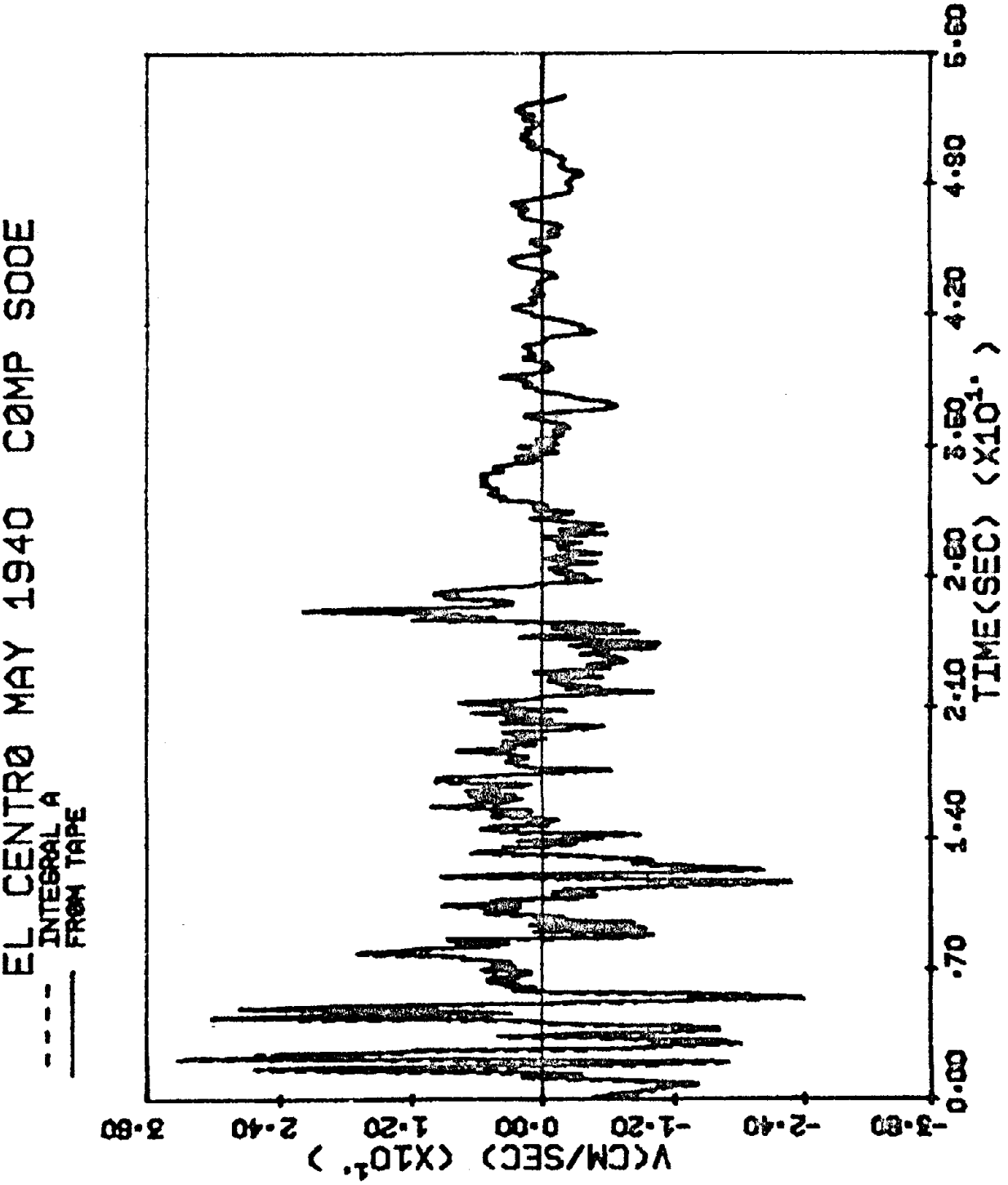
EL CENTRO MAY 1940 COMP S00E
INTEGRAL A
FROM TAPE
V(CM/SEC) (X10¹·)
-3.80
-2.40
-1.20
0.00
1.20
2.40
3.80
TIME(SEC) (X10¹·)
0.00
.70
1.40
2.10
2.80
3.50
4.20
4.90
5.60

FIG. 5

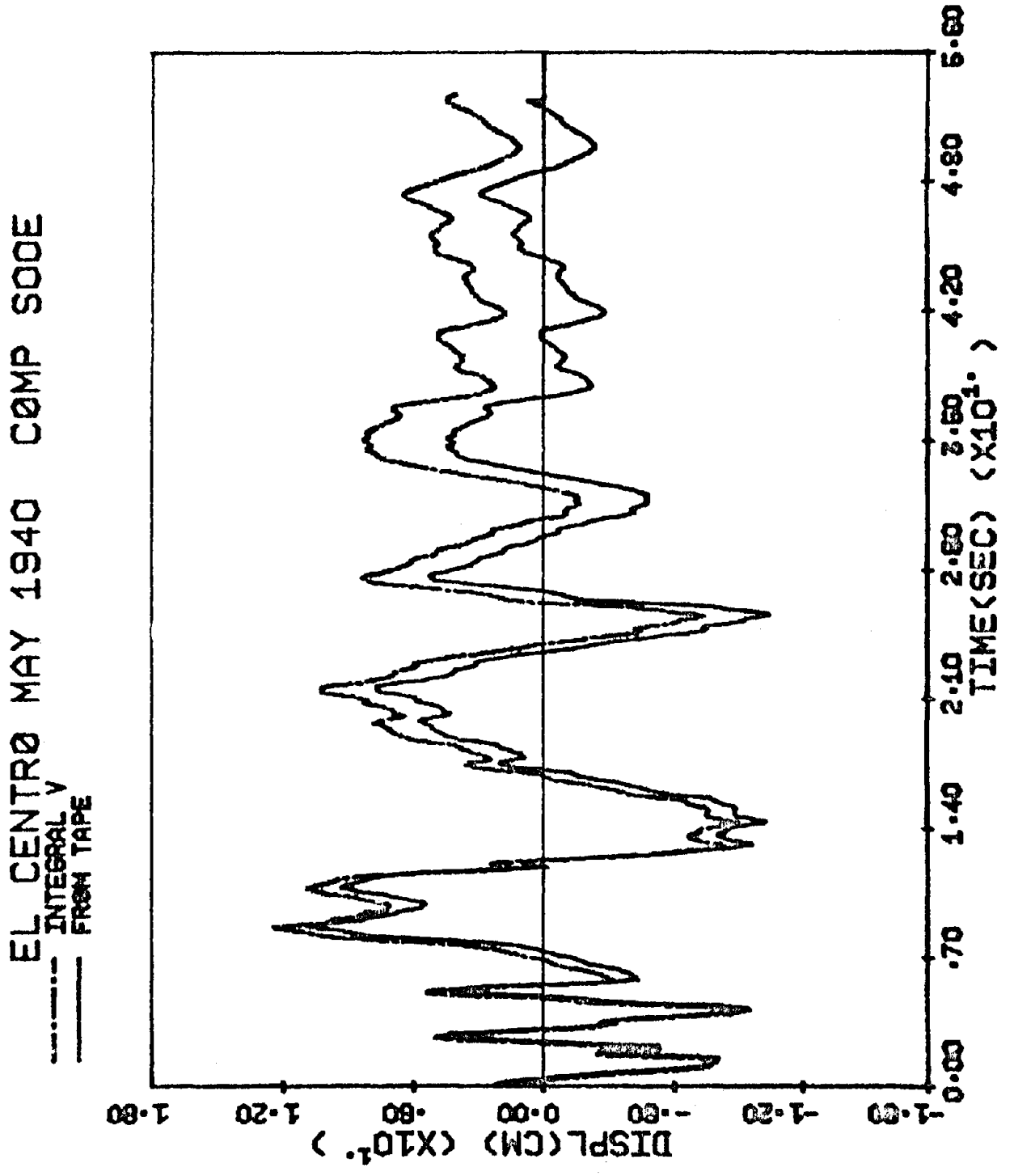
EL CENTRO MAY 1940 COMP SOOE
INTEGRAL V
FROM TAPE
DISPL(CM) (X10^1.)
TIME(SEC) (X10^1.)
-1.00
-1.20
-.60
0.00
.60
1.20
1.80
0.00
.70
1.40
2.10
2.80
3.50
4.20
4.90
5.60

FIG. 6

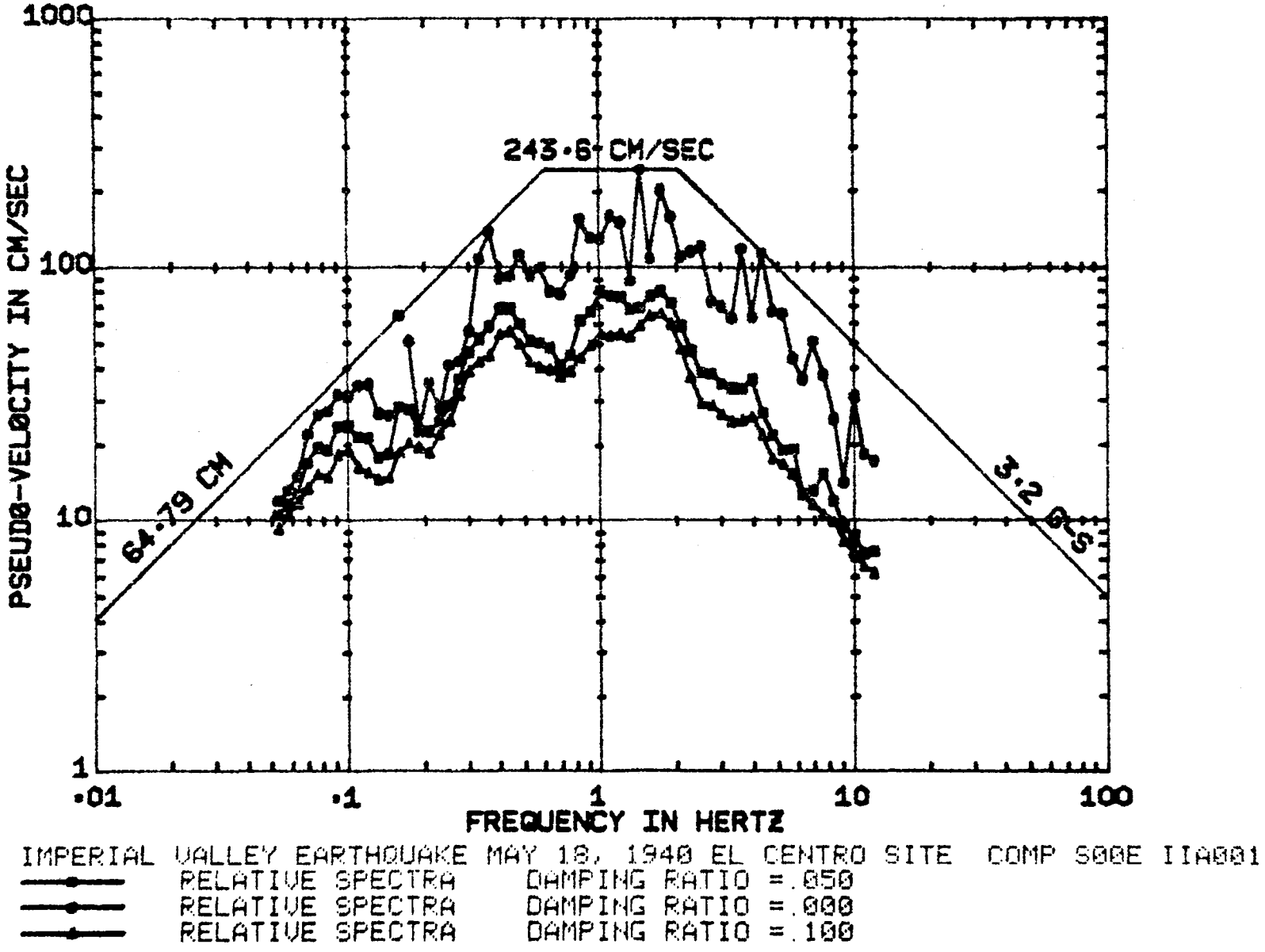
1000
100
10
1
PSEUDO-VELOCITY IN CM/SEC
243.6 CM/SEC
64.79 CM
3.2 SEC
.01
.1
1
10
100
FREQUENCY IN HERTZ
IMPERIAL VALLEY EARTHQUAKE MAY 18, 1940 EL CENTRO SITE COMP S00E IIA001
RELATIVE SPECTRA DAMPING RATIO =.050
RELATIVE SPECTRA DAMPING RATIO =.000
RELATIVE SPECTRA DAMPING RATIO =.100

FIG. 7

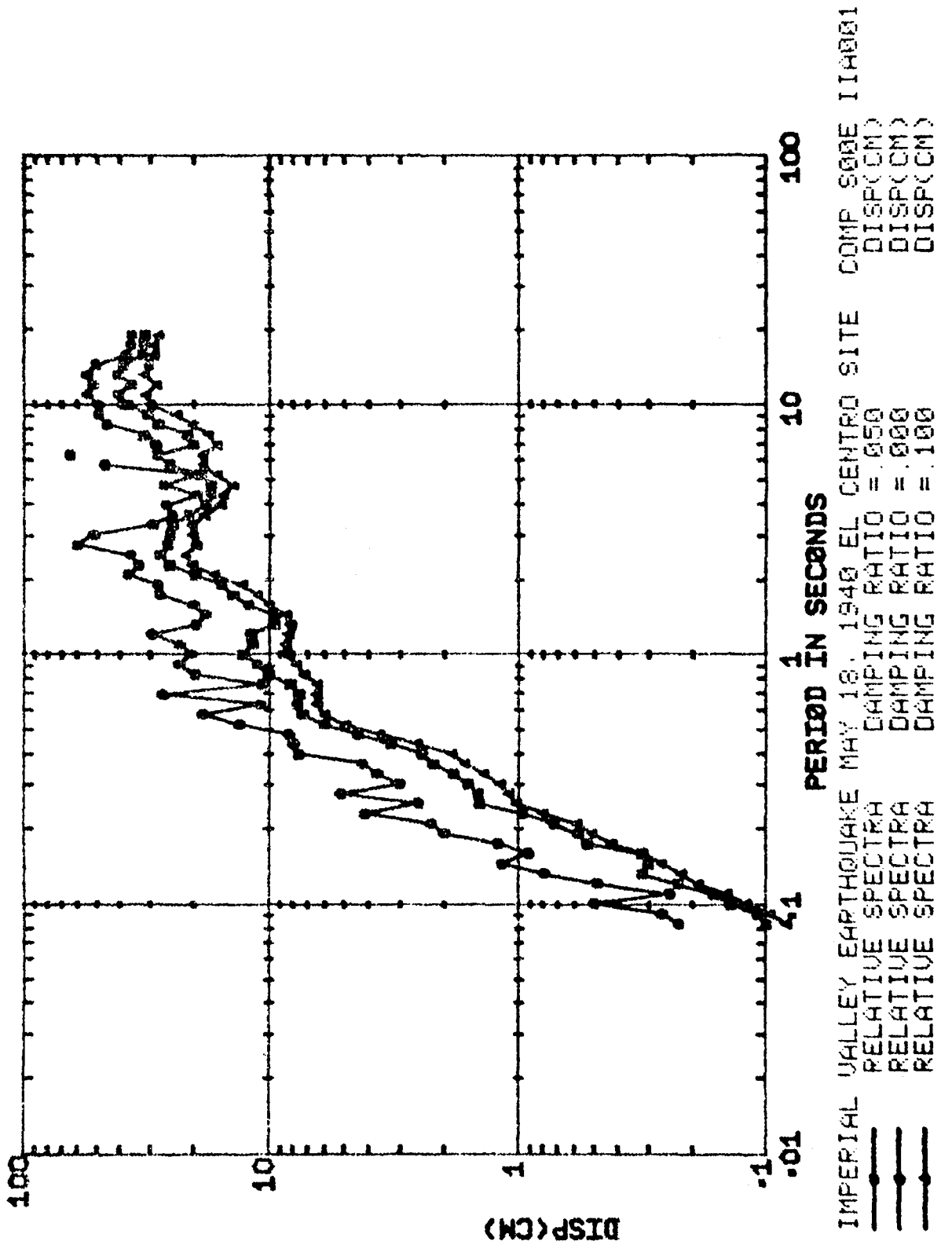
IMPERIAL VALLEY EARTHQUAKE MAY 18, 1940 EL CENTRO SITE COMP S00E II4001
RELATIVE SPECTRA DAMPING RATIO = .050 DISP(CM)
RELATIVE SPECTRA DAMPING RATIO = .000 DISP(CM)
RELATIVE SPECTRA DAMPING RATIO = .100 DISP(CM)
DISP(CM)
100
10
1
.1
.01
PERIOD IN SECONDS
.1
1
10
100

FIG. 8

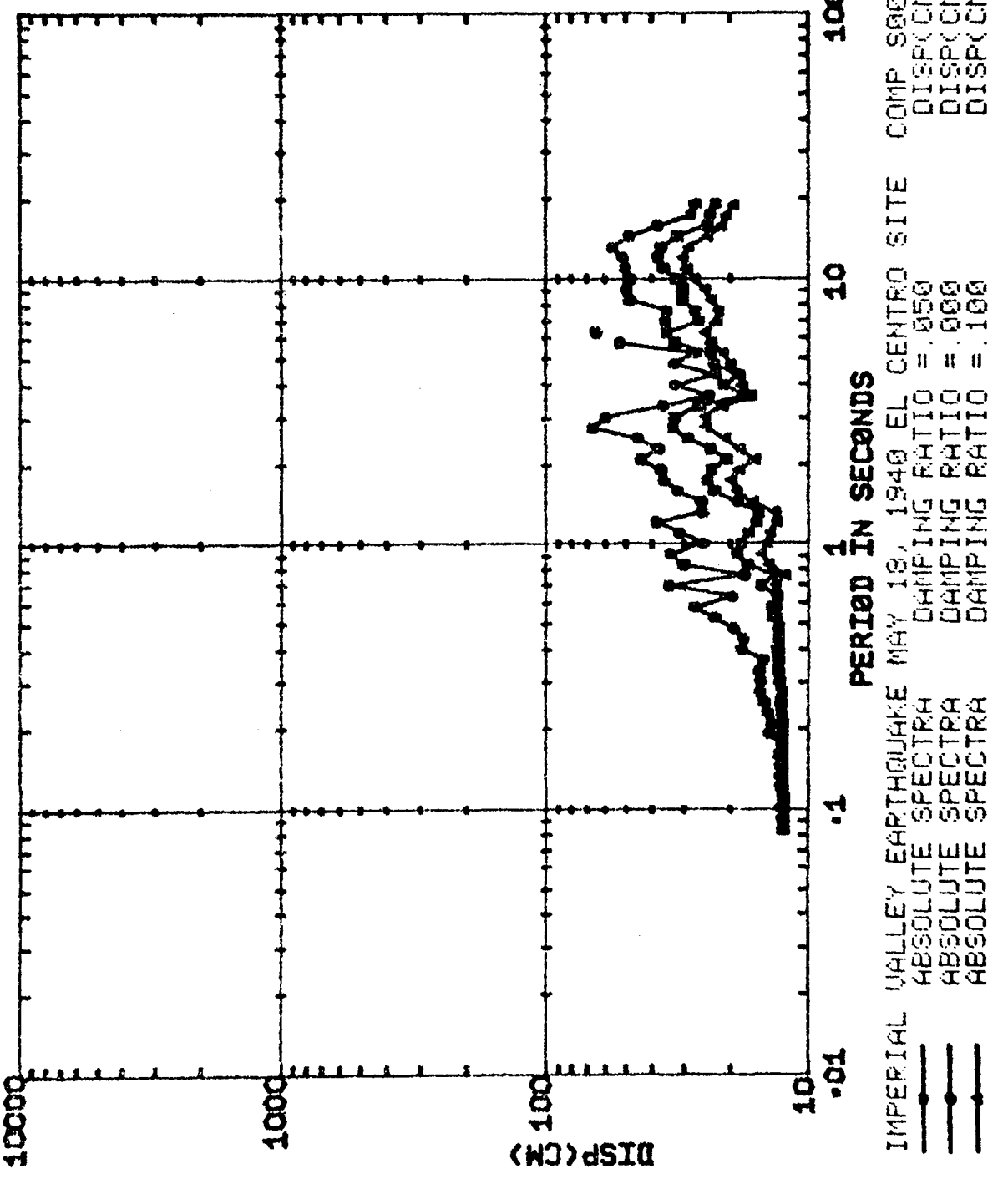
IMPERIAL VALLEY EARTHQUAKE MAY 18, 1940 EL CENTRO SITE COMP S00E II4001
ABSOLUTE SPECTRA DAMPING RATIO = .050 DISP(CM)
ABSOLUTE SPECTRA DAMPING RATIO = .000 DISP(CM)
ABSOLUTE SPECTRA DAMPING RATIO = .100 DISP(CM)
DISP(CM)
10000
1000
100
10
.01
.1
1
10
100
PERIOD IN SECONDS

FIG. 9

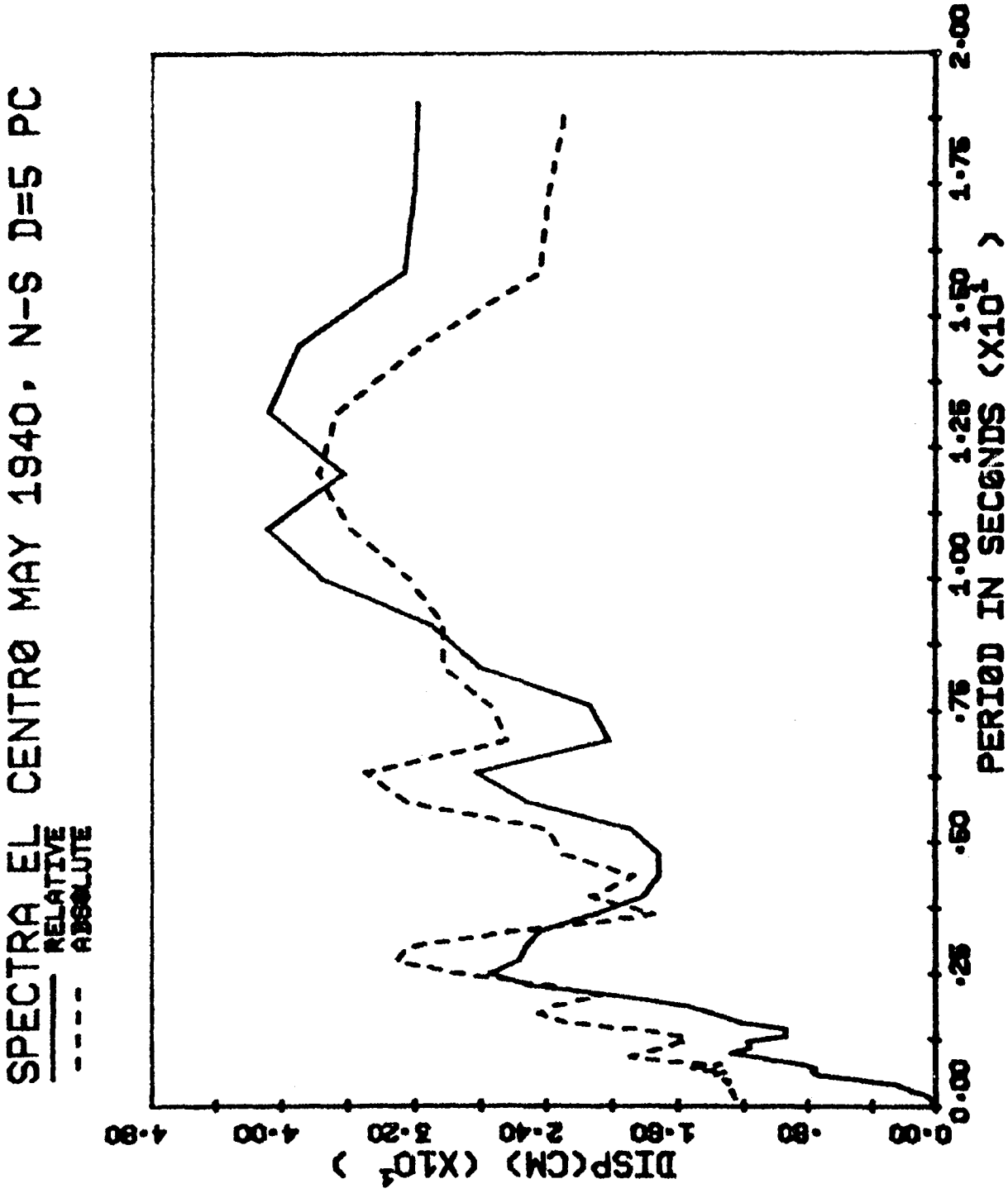
SPECTRA EL CENTRO MAY 1940, N-S D=5 PC
RELATIVE
ABSOLUTE
DISP(CM) (X10^{4})
PERIOD IN SECONDS (X10^{1})
0.00
.80
1.60
2.40
3.20
4.00
4.80
0.00
.25
.50
.75
1.00
1.25
1.50
1.75
2.00

FIG. 10

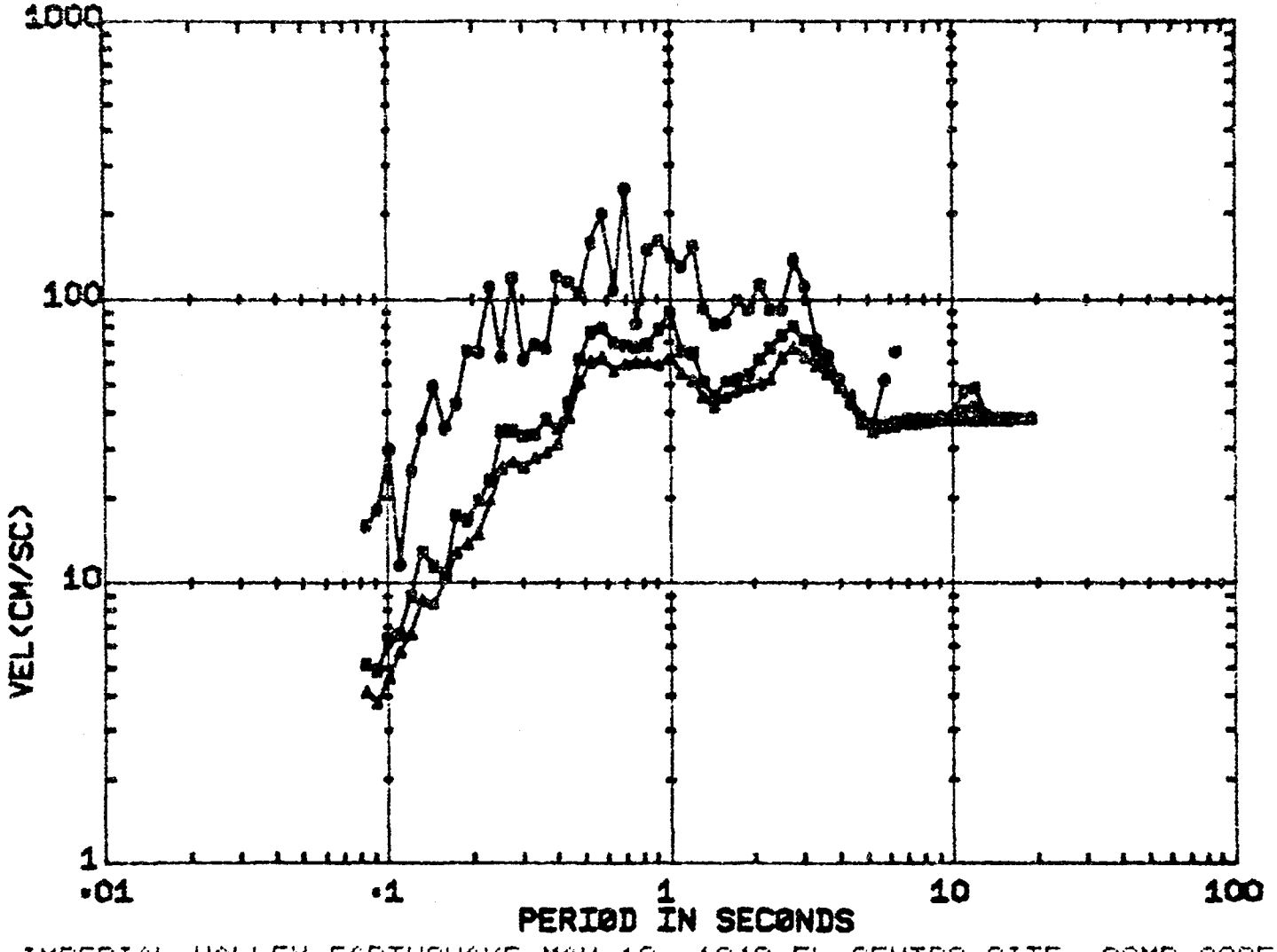

IMPERIAL VALLEY EARTHQUAKE MAY 18, 1940 EL CENTRO SITE COMP S00E IIA001

RELATIVE SPECTRA DAMPING RATIO = .050 VEL(CM/SC)

RELATIVE SPECTRA DAMPING RATIO = .000 VEL(CM/SC)

RELATIVE SPECTRA DAMPING RATIO = .100 VEL(CM/SC)

FIG. 11

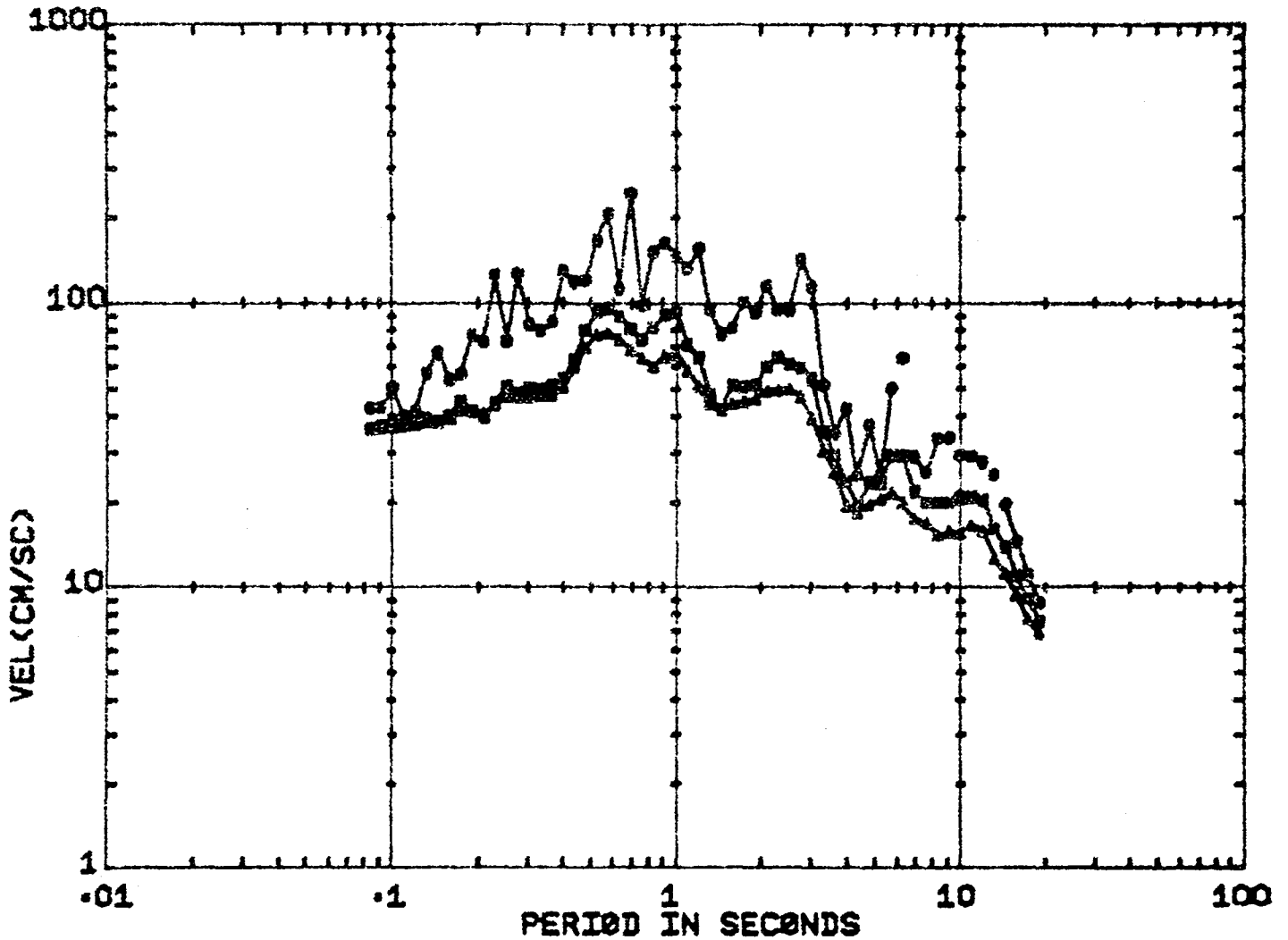
1000
100
10
1
VEL(CM/SC)
.01
.1
1
10
100
PERIØD IN SECØNDS
IMPERIAL VALLEY EARTHQUAKE MAY 18, 1940 EL CENTRO SITE COMP S00E IIA001
ABSOLUTE SPECTRA DAMPING RATIO =.050 VEL(CM/SC)
ABSOLUTE SPECTRA DAMPING RATIO =.000 VEL(CM/SC)
ABSOLUTE SPECTRA DAMPING RATIO =.100 VEL(CM/SC)

FIG. 12

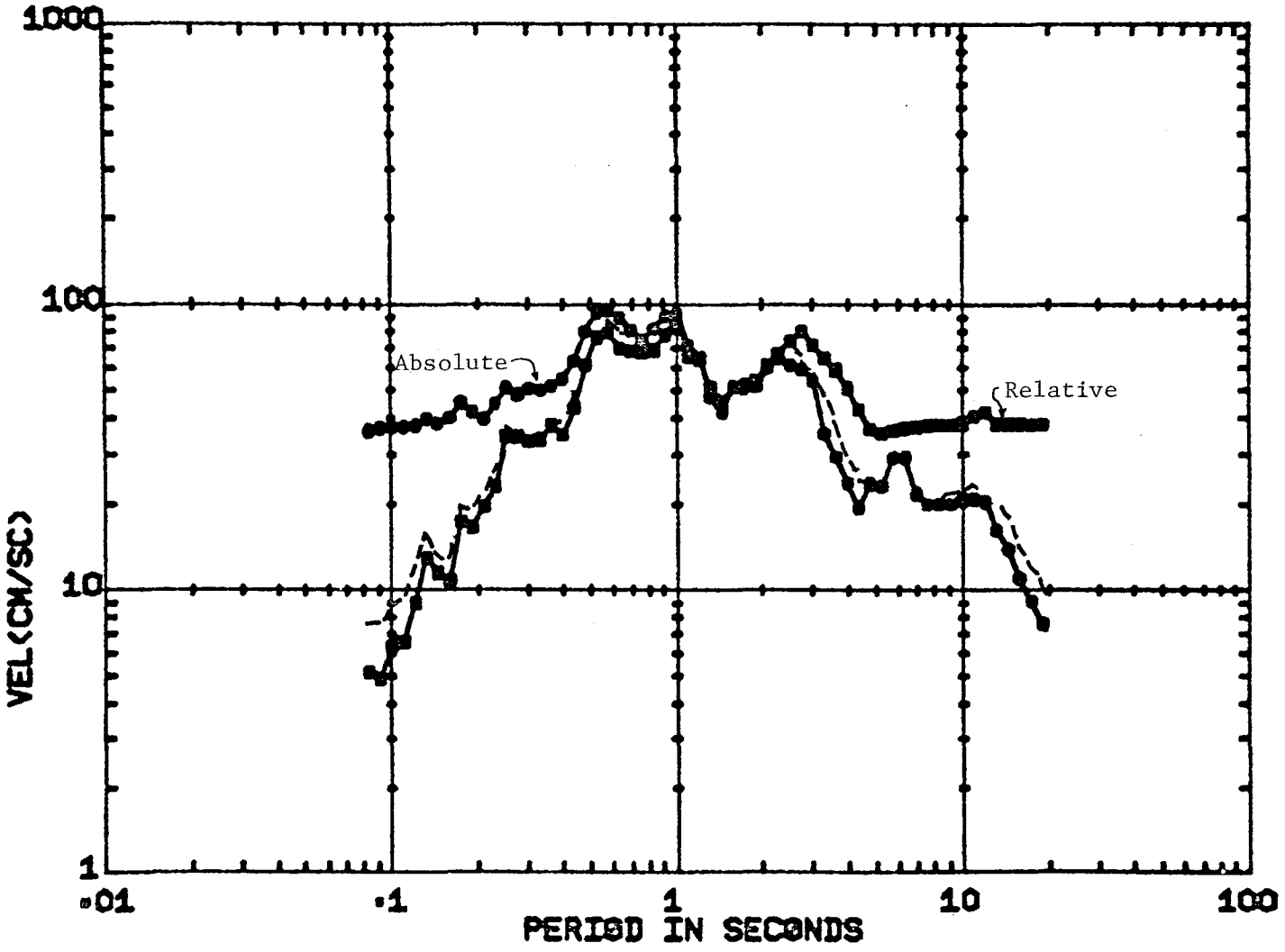
1000
100
10
1
VEL(CM/SC)
Absolute
Relative
.01
.1
1
10
100
PERIOD IN SECONDS
IMPERIAL VALLEY EARTHQUAKE MAY 18, 1940 EL CENTRO SITE COMP S00E IIA001
RELATIVE SPECTRA DAMPING RATIO =.050 VEL(CM/SC)
ABSOLUTE SPECTRA DAMPING RATIO =.050 VEL(CM/SC)
PSEUDO VELOCITY

FIG. 13

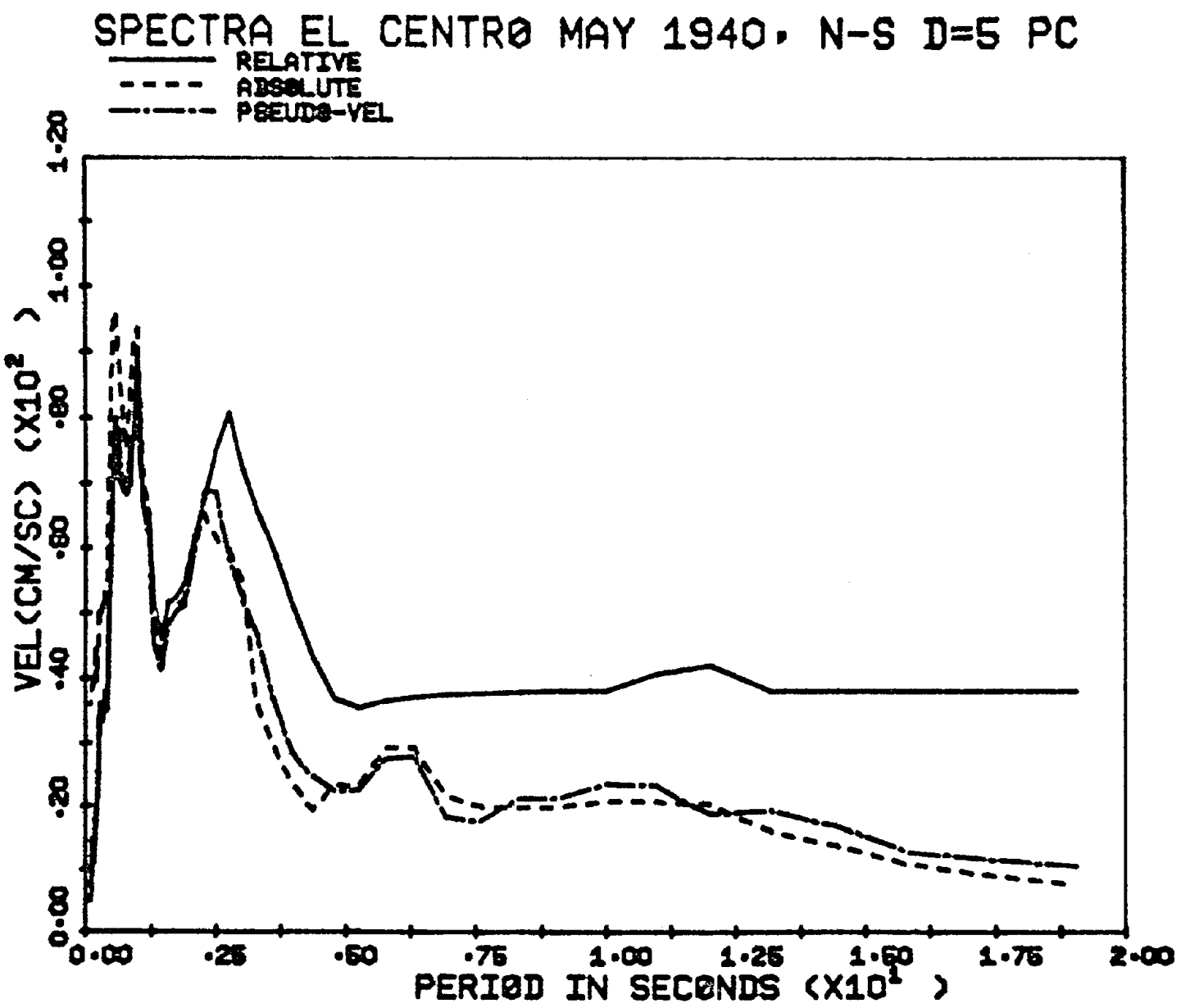
SPECTRA EL CENTRØ MAY 1940, N-S D=5 PC
RELATIVE
ABSØLUTE
PSEUDØ-VEL
VEL(CM/SC) (X10²)
0.00
.20
.40
.60
.80
1.00
1.20
0.00
.25
.50
.75
1.00
1.25
1.50
1.75
2.00
PERIØD IN SECØNDS (X10¹)

FIG. 14

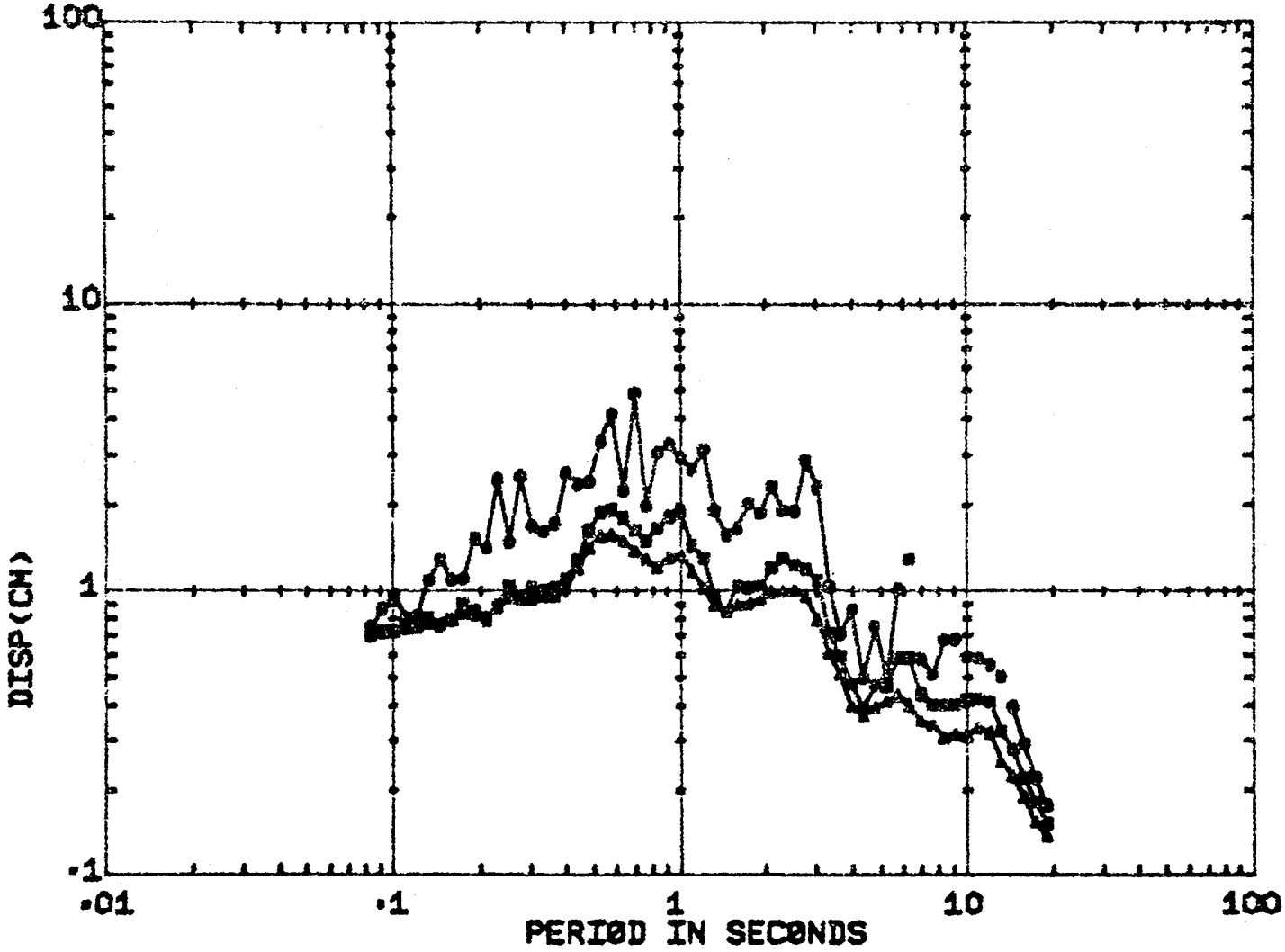

IMPERIAL VALLEY EARTHQUAKE MAY 18, 1940 EL CENTRO SITE COMP S00E IIA001
DIFFERENTIAL SPECTRA WITH DT = .020 SEC DAMPING RATIO =.050
DIFFERENTIAL SPECTRA WITH DT = .020 SEC DAMPING RATIO =.000
DIFFERENTIAL SPECTRA WITH DT = .020 SEC DAMPING RATIO =.100

FIG. 15

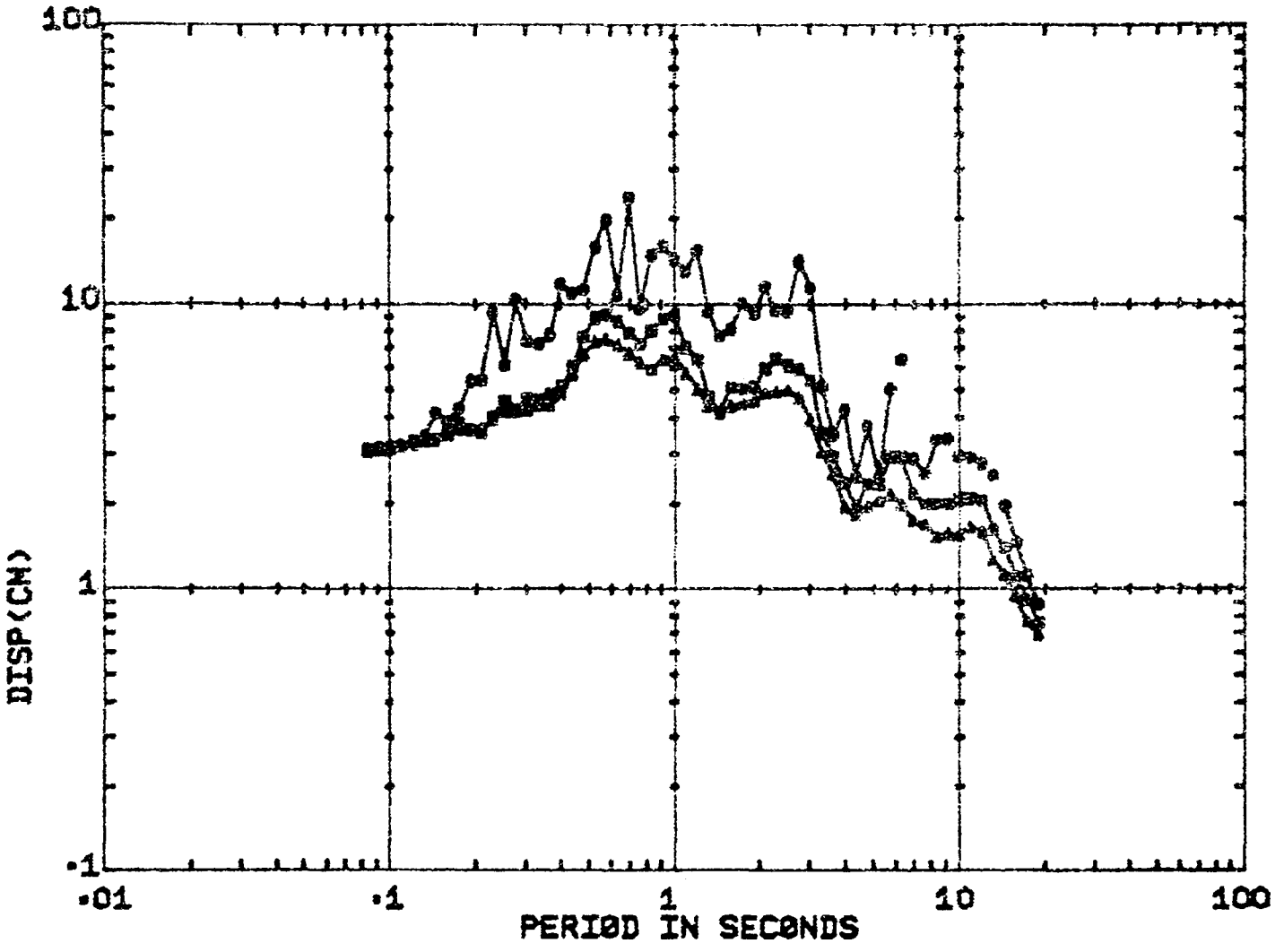

IMPERIAL VALLEY EARTHQUAKE MAY 18, 1940 EL CENTRO SITE COMP S00E IIA001
DIFFERENTIAL SPECTRA WITH DT = .100 SEC DAMPING RATIO =.050
DIFFERENTIAL SPECTRA WITH DT = .100 SEC DAMPING RATIO =.000
DIFFERENTIAL SPECTRA WITH DT = .100 SEC DAMPING RATIO =.100

FIG. 16

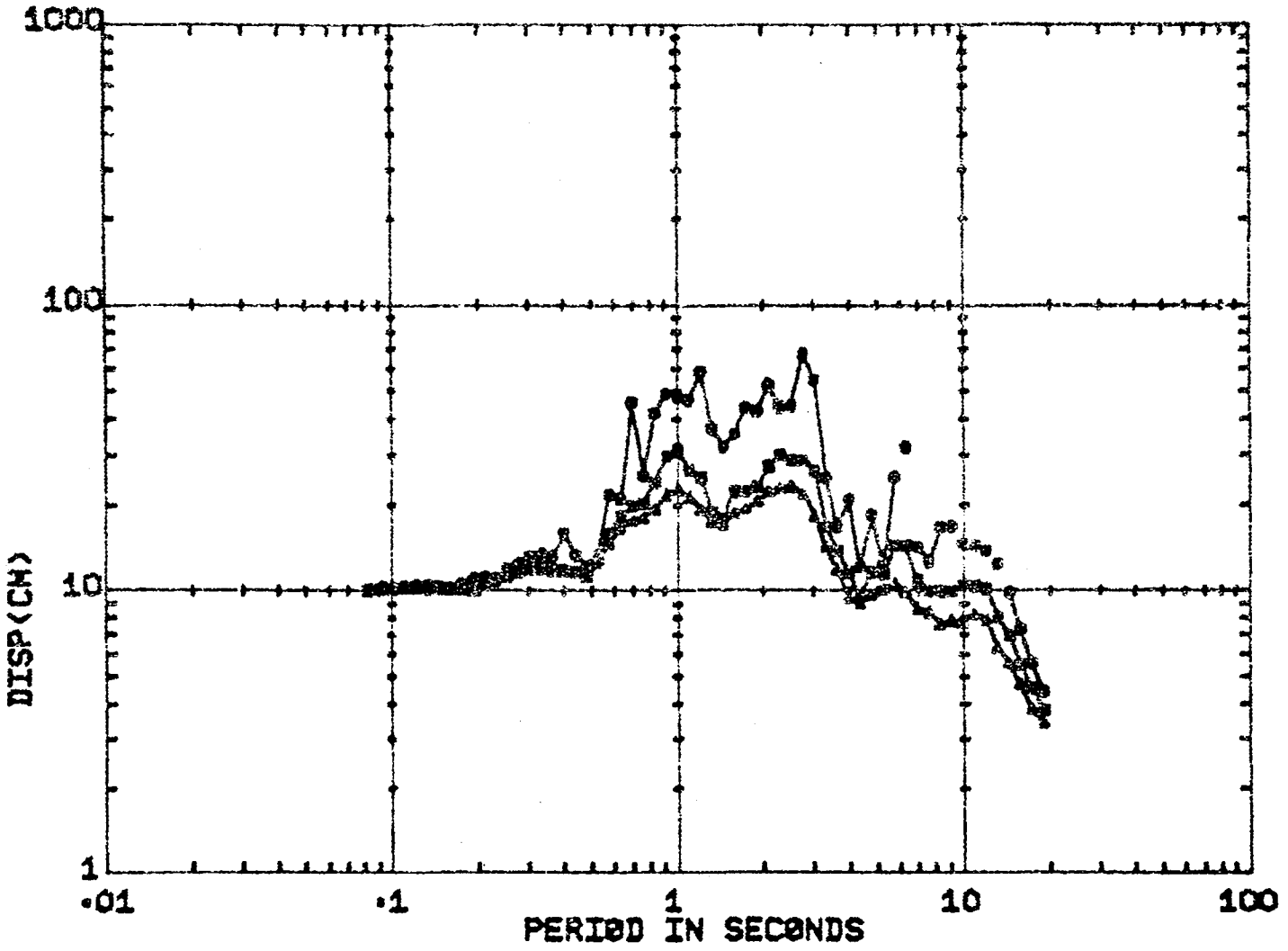

IMPERIAL VALLEY EARTHQUAKE MAY 18, 1940 EL CENTRO SITE COMP S00E IIA001

DIFFERENTIAL SPECTRA WITH DT = .500 SEC DAMPING RATIO = .050

DIFFERENTIAL SPECTRA WITH DT = .500 SEC DAMPING RATIO = .000

DIFFERENTIAL SPECTRA WITH DT = .500 SEC DAMPING RATIO = .100

FIG. 17

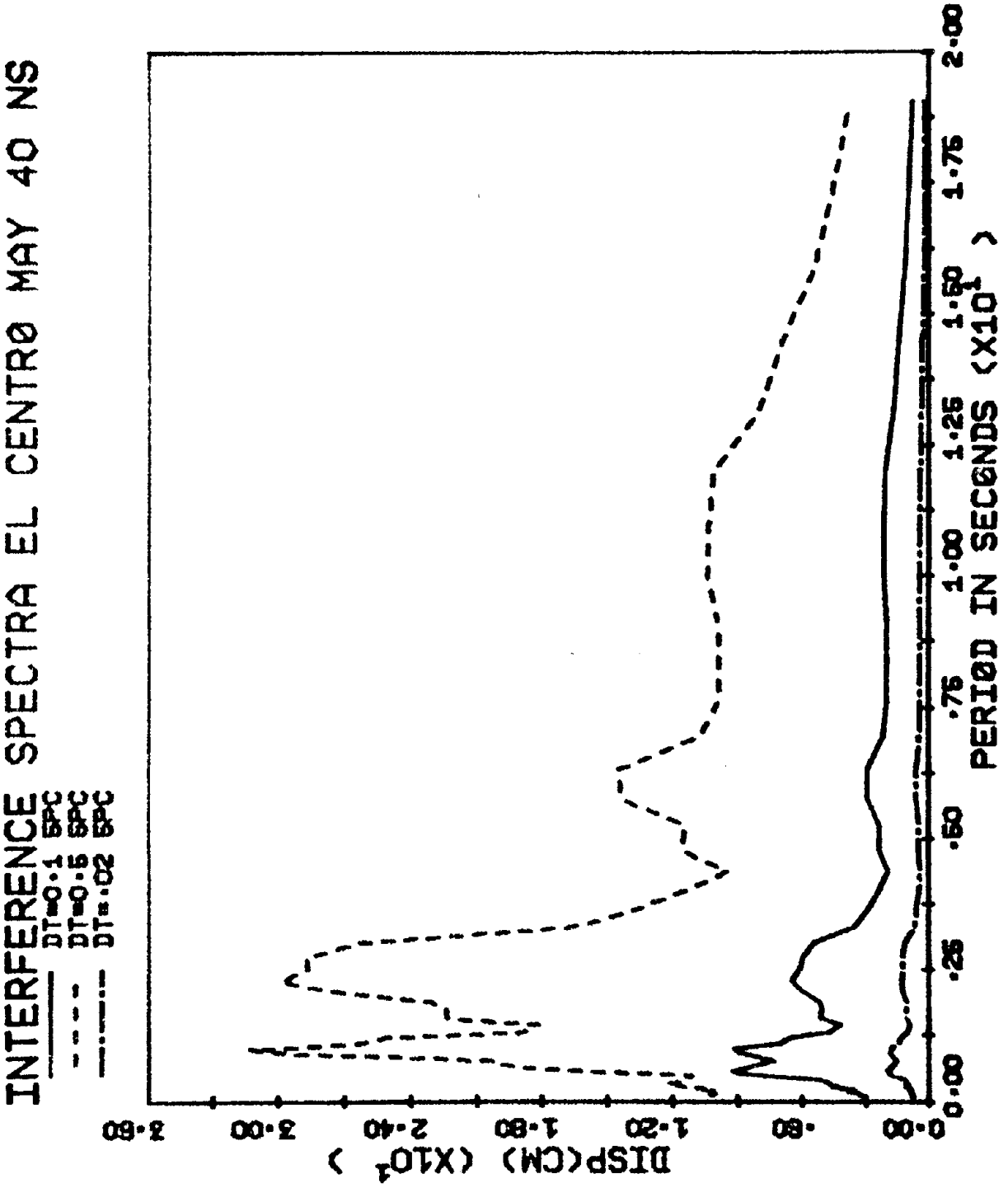
INTERFERENCE SPECTRA EL CENTRO MAY 40 NS
DT=0.1 SPC
DT=0.5 SPC
DT=.02 SPC
DISP(CM) (X10⁴)
PERIOD IN SECONDS (X10⁻¹)
0.00
.80
1.20
1.80
2.40
3.00
3.60
.25
.50
.75
1.00
1.25
1.50
1.75
2.00

FIG. 18

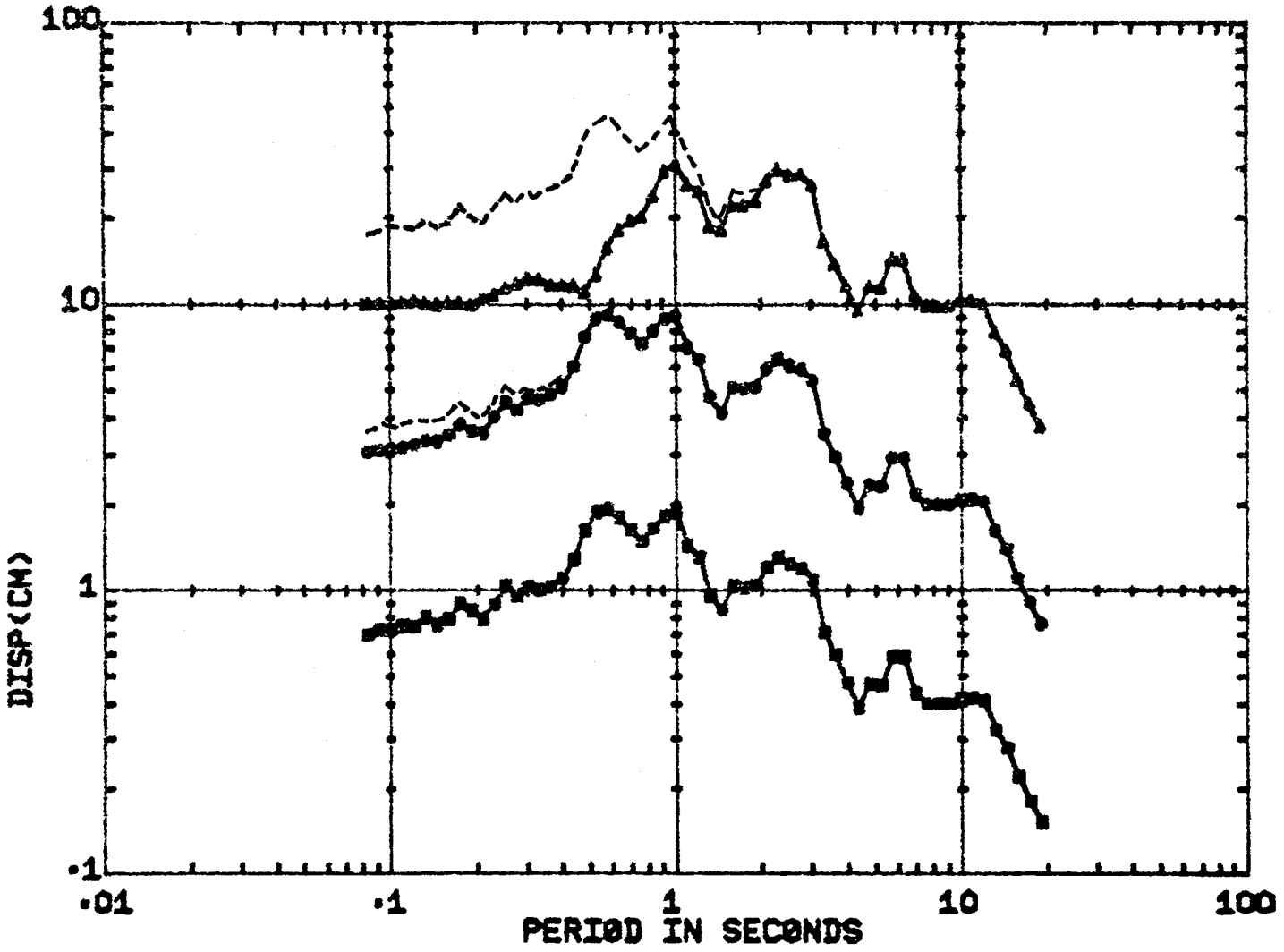

IMPERIAL VALLEY EARTHQUAKE MAY 18, 1940 EL CENTRO SITE COMP S00E II A001

DIFFERENTIAL SPECTRA WITH DT = .020 SEC DAMPING RATIO = .050

DIFFERENTIAL SPECTRA WITH DT = .100 SEC DAMPING RATIO = .050

DIFFERENTIAL SPECTRA WITH DT = .500 SEC DAMPING RATIO = .050

ABSOLUTE VELOCITY SPECTRA × Δt

FIG. 19

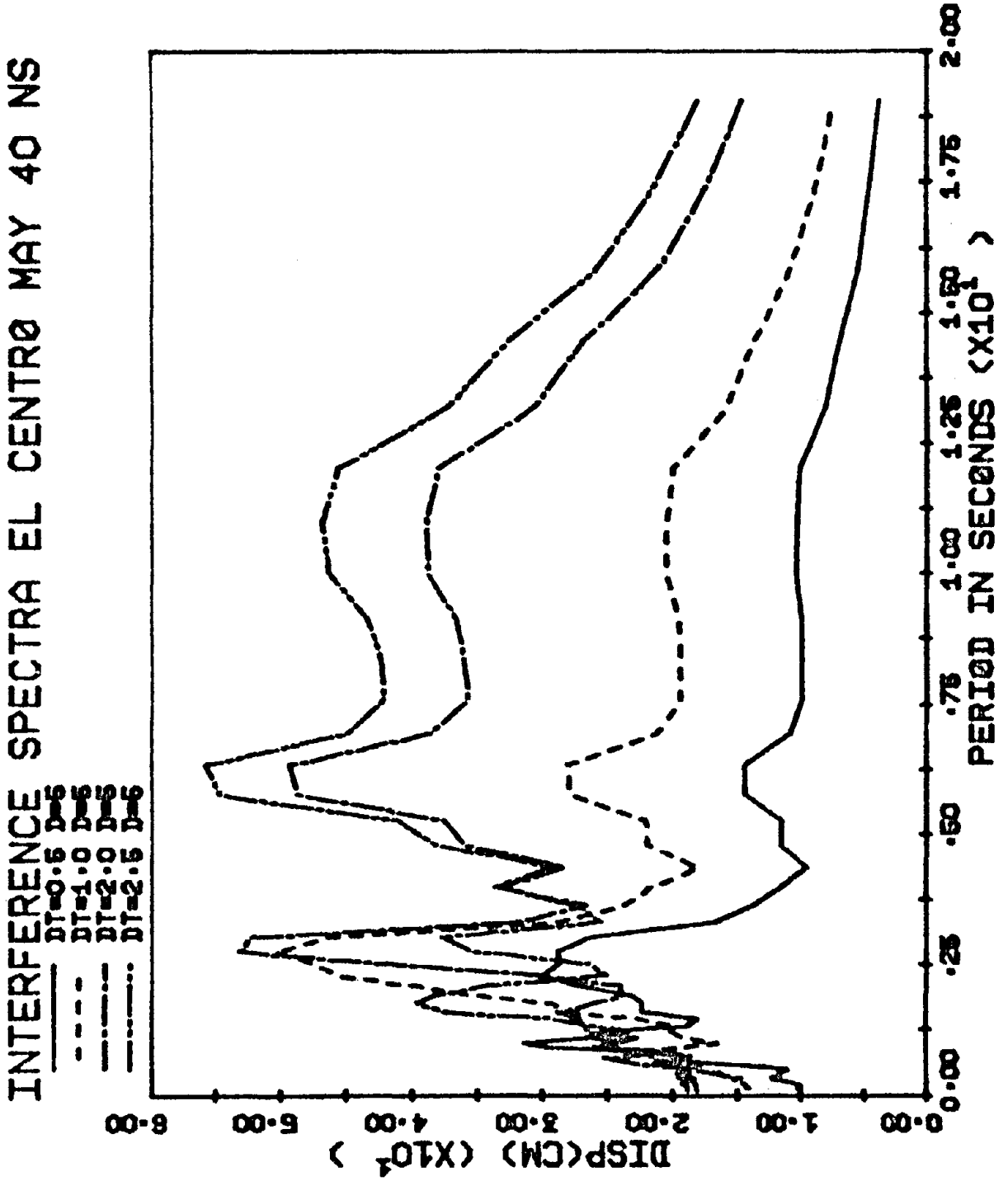
INTERFERENCE SPECTRA EL CENTRØ MAY 40 NS
DT=0.5
DT=1.0
DT=2.0
DT=2.5
DISP(CM) (X10⁴)
PERIØD IN SECØNDS (X10¹)
0.00
.25
.50
.75
1.00
1.25
1.50
1.75
2.00
1.00
2.00
3.00
4.00
5.00
6.00

FIG. 20

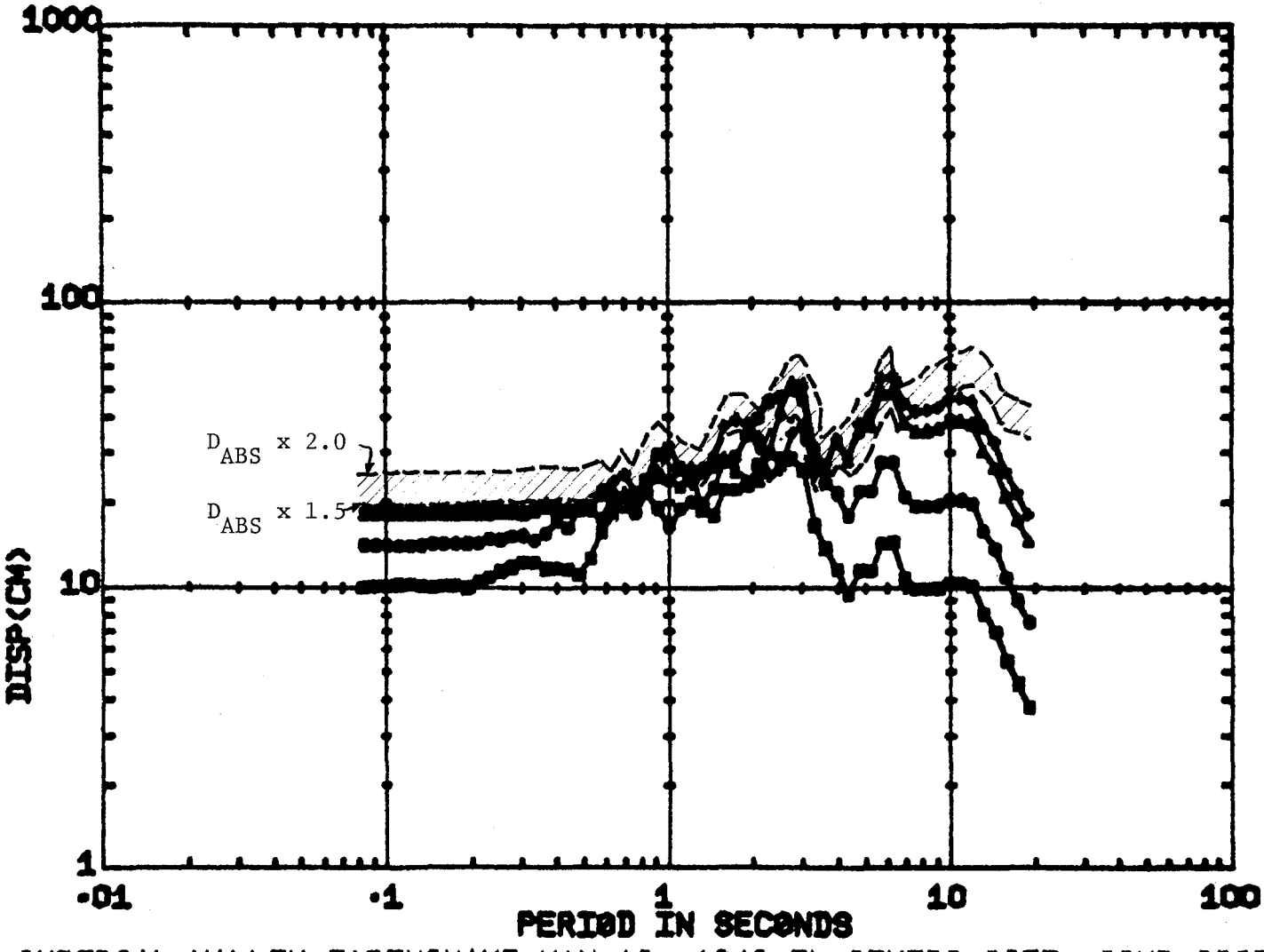

IMPERIAL VALLEY EARTHQUAKE MAY 18, 1940 EL CENTRO SITE COMP S00E IIA001

DIFFERENTIAL SPECTRA WITH DT = .500 SEC DAMPING RATIO =.050
DIFFERENTIAL SPECTRA WITH DT = 1.000 SEC DAMPING RATIO =.050
DIFFERENTIAL SPECTRA WITH DT = 2.000 SEC DAMPING RATIO =.050
DIFFERENTIAL SPECTRA WITH DT = 2.500 SEC DAMPING RATIO =.050

FIG. 21

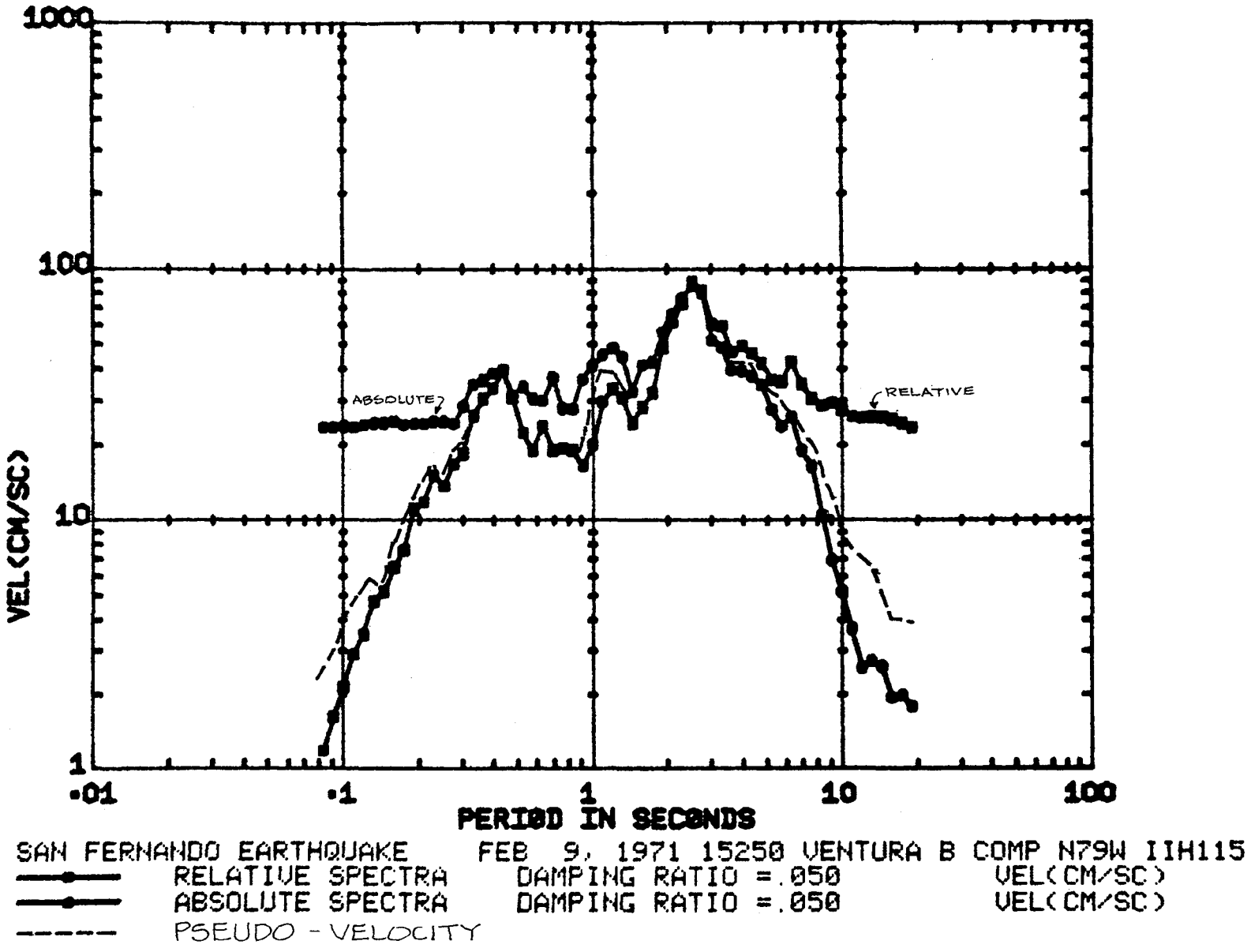
1000
100
10
1
VEL(CM/SC)
.01
.1
1
10
100
PERIOD IN SECONDS
ABSOLUTE
RELATIVE
SAN FERNANDO EARTHQUAKE FEB 9, 1971 15250 VENTURA B COMP N79W IIH115
RELATIVE SPECTRA DAMPING RATIO = .050 VEL(CM/SC)
ABSOLUTE SPECTRA DAMPING RATIO = .050 VEL(CM/SC)
PSEUDO - VELOCITY

FIG. 22

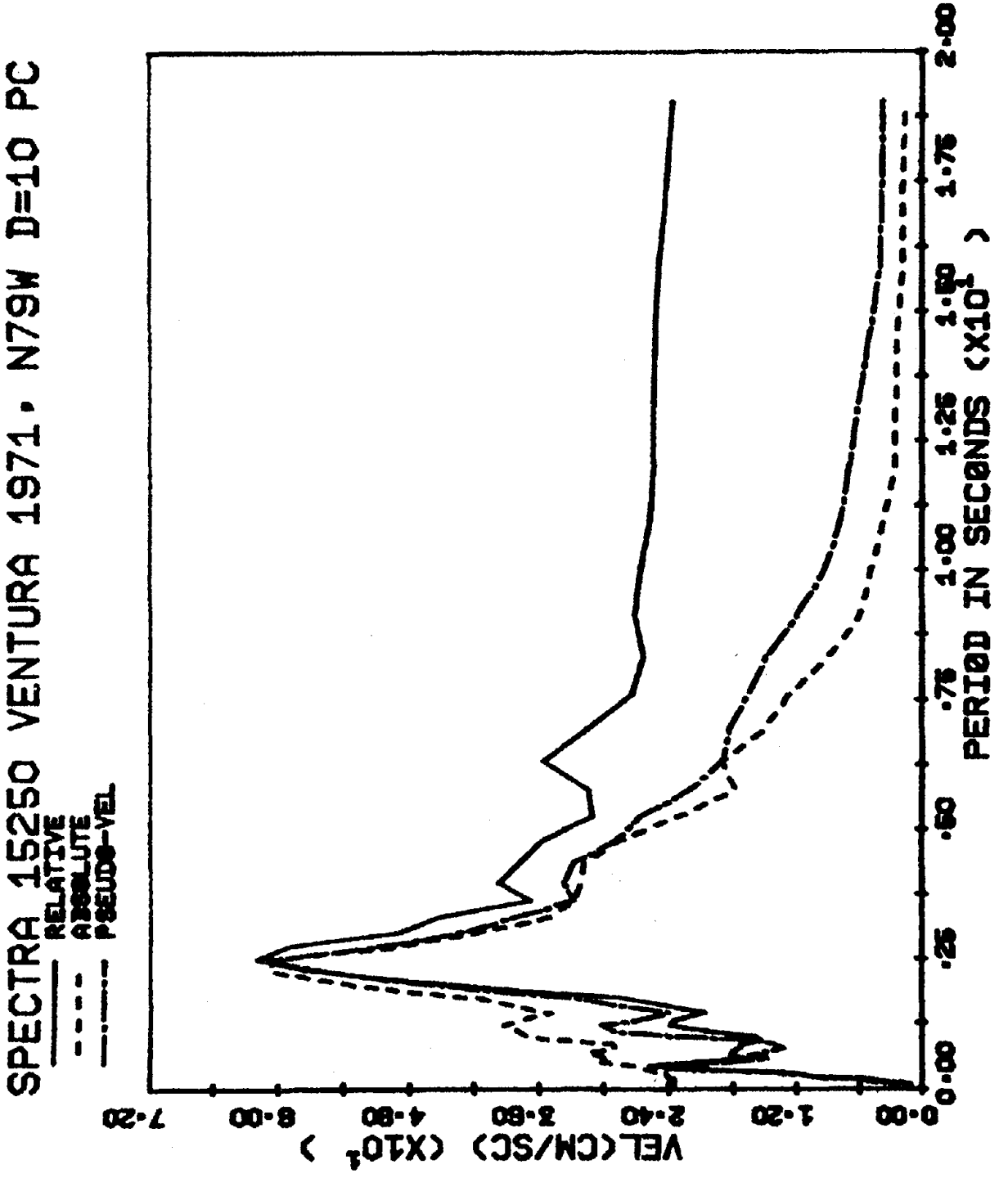
SPECTRA 15250 VENTURA 1971, N79W D=10 PC
RELATIVE
ABSOLUTE
PSEUDO-VEL
VEL(CM/SC) (X10¹)
0.00
1.20
2.40
3.60
4.80
6.00
7.20
0.00
.25
.50
.75
1.00
1.25
1.50
1.75
2.00
PERIOD IN SECONDS (X10⁻¹)

FIG. 23

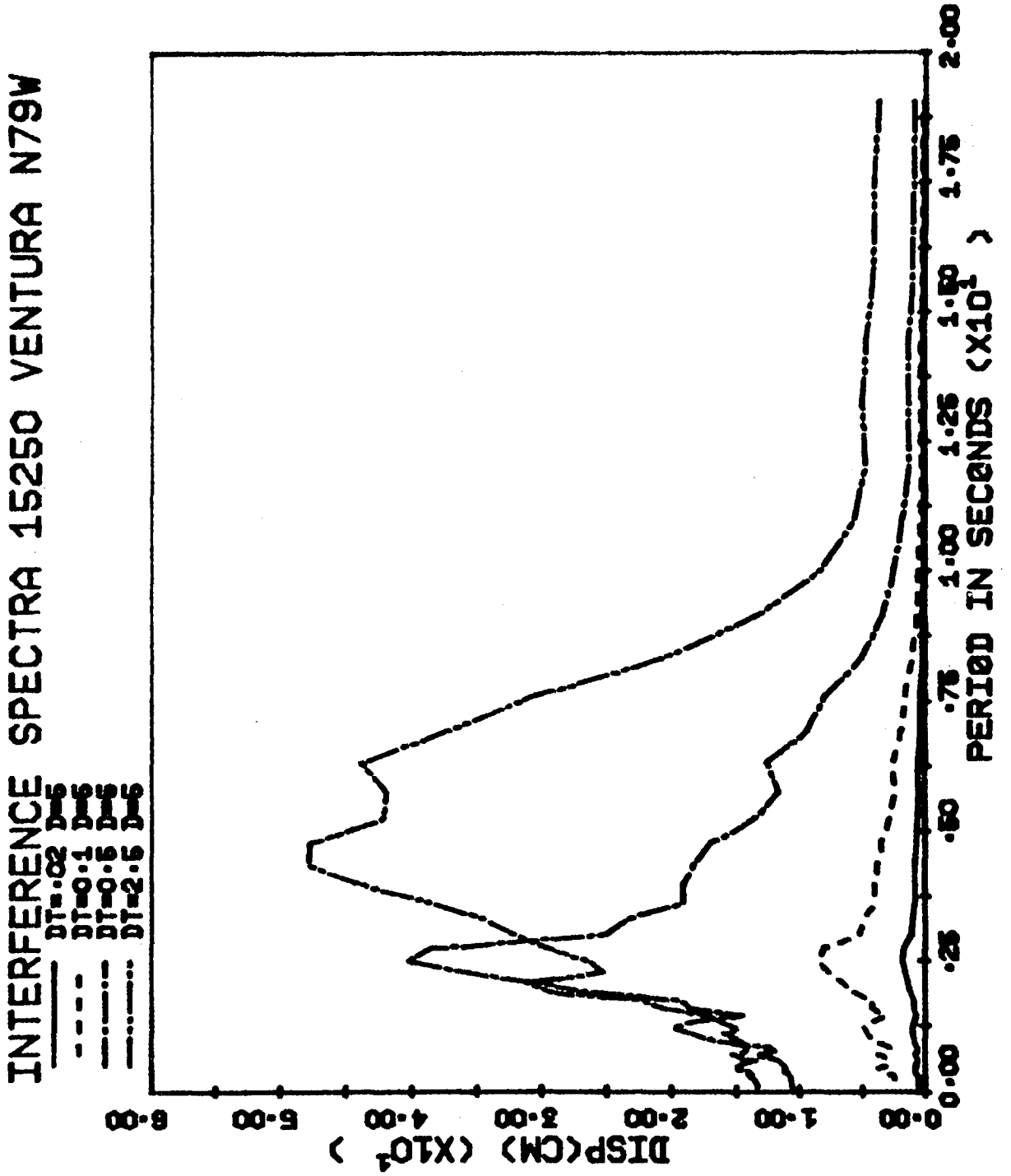
INTERFERENCE SPECTRA 15250 VENTURA N79W
DT=.02 D=5
DT=0.1 D=5
DT=0.5 D=5
DT=2.5 D=5
DISP(CM) (X10⁻⁴)
0.00
1.00
2.00
3.00
4.00
5.00
6.00
.00
.25
.50
.75
1.00
1.25
1.50
1.75
2.00
PERIOD IN SECONDS (X10⁻¹)

FIG. 24

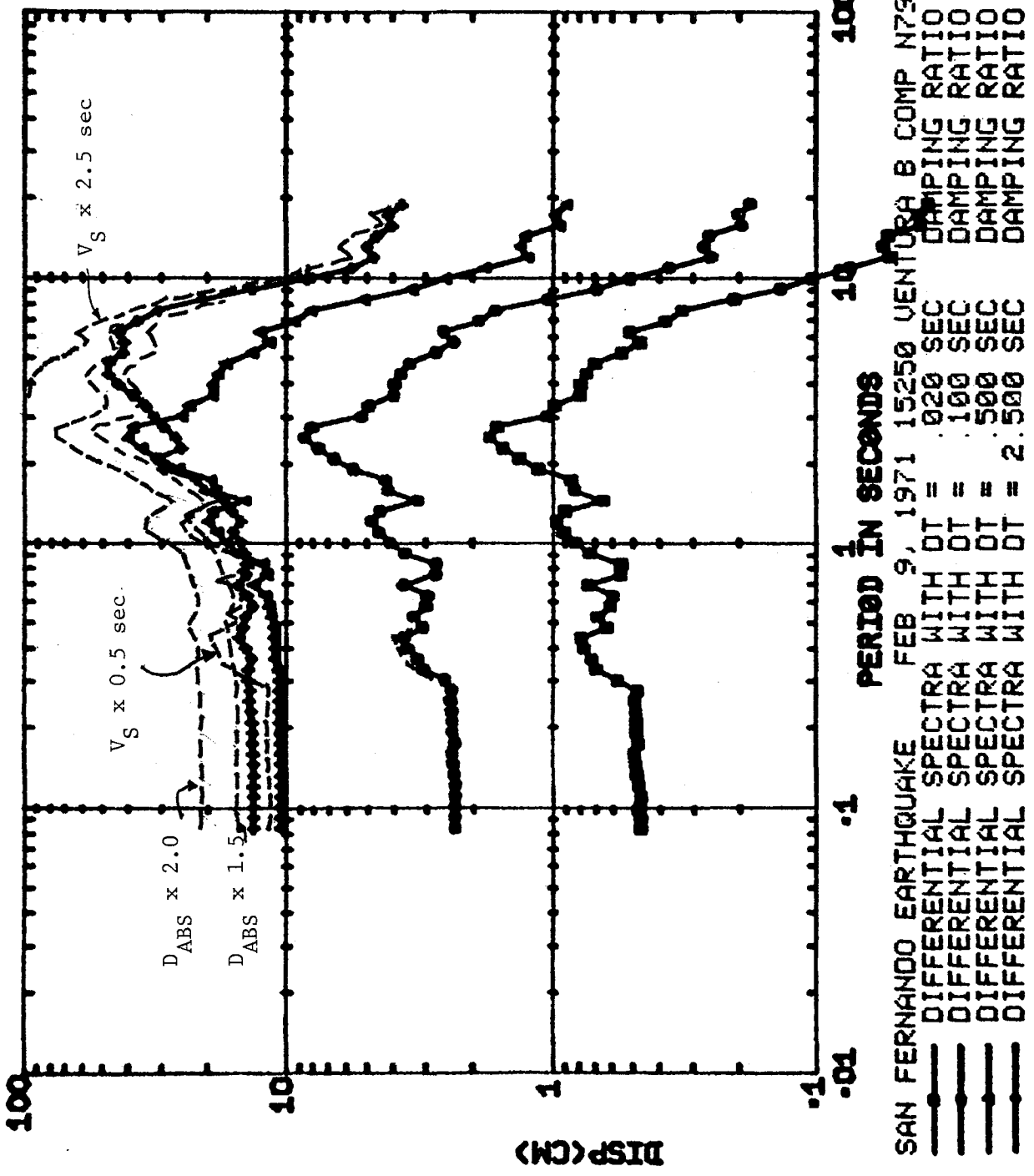
SAN FERNANDO EARTHQUAKE FEB 9, 1971 15250 VENTURA B COMP N79W 11H115
DIFFERENTIAL SPECTRA WITH DT = .020 SEC DAMPING RATIO =.050
DIFFERENTIAL SPECTRA WITH DT = .100 SEC DAMPING RATIO =.050
DIFFERENTIAL SPECTRA WITH DT = .500 SEC DAMPING RATIO =.050
DIFFERENTIAL SPECTRA WITH DT = 2.500 SEC DAMPING RATIO =.050
PERIOD IN SECONDS
DISP(CM)
100
10
1
.1
.01
.1
1
10
100
V_S x 2.5 sec
V_S x 0.5 sec
D_{ABS} x 2.0
D_{ABS} x 1.5

FIG. 25